

**The ribosomal RNA gene repeat is transported to the
nuclear pore complex for the repeat maintenance**

Eri Unozawa

Doctor of Philosophy

Department of Genetics

School of Life Science

SOKENDAI (THE GRADUATE UNIVERSITY FOR ADVANCED STUDIES)

2015

Contents

1. Abstract	3~5
2. Introduction	6~10
3. Results	11~21
3.1 Tel1 is involved in recombination repair for DSB caused by Fob1 at the RFB	
3.2 The rDNA relocates to the NPC in a Fob1-dependent manner	
3.3 Factors for anchoring the HO-induced DSB to the NPC are also required for the transportation of the rDNA to the NPC	
3.4 Condensin recruiting factors to the RFB are required for the transportation of the rDNA to the NPC	
3.5 The transportation of the rDNA to the NPC affects rDNA stability	
3.6 A histone variant is not involved in the transportation of the rDNA to the NPC	
3.7 Ubiquitin ligases are related to the transportation of rDNA to the NPC	
3.8 The rDNA is transported not only to the NPC but also to Mps3	
2.9 The RFB is not always required for the transportation	
4. Discussion	22~31
5. Acknowledgements	32
6. Materials and Methods	33~44
7. References	45~51
8. Tables and Figures	52~

1. Abstract

The broken chromosomal DNAs need to be repaired correctly. The broken ends are usually repaired by DNA repair systems. If the broken ends are not repaired properly, they may cause rearrangement of the genome, such as deletion, translocation and amplification. These rearrangements could lead to diseases including cancer and cellular senescence. Therefore, it is important for cells to repair the broken ends correctly.

In DNA replication, the replication fork is stalled at a replication fork blocking site. The stalled replication fork possibly leads to the broken end at the site. The ribosomal RNA gene repeats (rDNA) in the budding yeast *Saccharomyces cerevisiae* has a replication fork block site in which gene amplification recombination is induced. By the recombination, rDNA repeat number is recovered through the DNA double-strand break (DSB) repair pathway. In this system, DSB that is induced by Fob1 at the replication fork barrier (RFB) site is repaired by unequal sister-chromatid recombination. As the result, the some repeats are replicated twice to increase the repeat number. When the broken end recombines with improper repeating unit, deletional recombination or reorganization of the repeat may occur and the rDNA becomes unstable. Therefore, the rDNA is expected to have a system in which the recombination is properly regulated.

In our laboratory, through screening of genes that reduce rDNA stability, *TELI* was

identified. *TEL1* is an ortholog of ATM in mammals. Tel1 has several functions, such as telomere maintenance, checkpoint control, and DSB repair.

First, to confirm the change of repeat number in the rDNA, Chr.XII that has the huge rDNA repeat was analyzed by pulsed-field gel electrophoresis (CHEF). As the result, in the *tell* mutant, the rDNA was highly unstable to compare with that in the wild-type. Next, I investigated whether the function of Tel1 in the rDNA is dependent on Fob1 or not. When both *TEL1* and *FOB1* were deleted, the rDNA was stable. Thereby suggesting that Tel1 is involved in recombination repair for DSB caused by Fob1 at the RFB.

Tel1 is also known to be involved in the transportation of unrepairable DSB of non-rDNA to the NPC. However, the significance of the system is not revealed. We speculated that the rDNA is also isolated near the NPC and prevented recombination with improper copies. Our research purposes were to uncover whether the rDNA is translocated to the nuclear pore complex and to identify genes that are related to the translocation. If Tel1 is related to translocation of the rDNA to the NPC, it will be an important function of Tel1 to maintain the rDNA.

To know whether the transportation system exists in the rDNA region, I performed CHIP assay and investigated the localization of the rDNA. As the result, the rDNA is surely located around the NPC. On the other hand, the pore localization of the rDNA is decreased in the *fob1* mutant. In the *fob1* mutant, as DSB is not induced, I speculate the Fob1-dependent DSB is

necessary for translocation of the rDNA to the NPC. Moreover, the rDNA association with the NPC is decreased in the *tell* mutant.

The DSB translocation of non-rDNA region was shown in an artificial system that an unreparable DSB is induced by HO endonuclease without any template for repair in the mating type locus on the Chr III. On the other hand, DSB in the rDNA is induced in the natural process. In the replication of the rDNA, the broken end occurs at the RFB site by blocking the replication fork machinery. Hence I expected the some factors for the transportation of the rDNA to the NPC are different from those for the anchoring the artificial DSB to the NPC. I focused on factors that function in both the rDNA and the nuclear membrane. By CHIP assay, I found that the condensin recruiting factors to the RFB are necessary for the transportation of the rDNA to the NPC.

As for the biological meaning of the rDNA translocation, I speculate that DSB should be isolated from other repeats to avoid improper recombination. Moreover, we assume that the localization is required for the rDNA condensation that is important for chromosome segregation and repeats maintenance.

2. Introduction

DNA has an important role for inheriting genetic information to the next generation. Nevertheless, DNA is constantly under threat of change by break. DNA double-strand breaks (DSBs) have serious effects to genome integrity if they are not repaired properly. Unrepaired DSBs lead to loss of genetic material, chromosomal duplications / translocations and carcinogenesis (Adkins *et al.*, 2013). The radiation, such as X-rays or gamma-rays, is direct external causes to induce DSB. DSB is also occurred by inhibition of replication fork progression. DSB is commonly repaired by homologous recombination (HR) or non-homologous end joining (NHEJ). These repair pathways are relatively conserved to higher eukaryotes. It means that DSB repair is important for life existence.

The ribosomal RNA gene cluster (rDNA) in budding yeast is an extreme repeat domain that is well-studied in eukaryotic cells. In *S. cerevisiae*, the rDNA is located on chromosome XII (Fig. 1). The rDNA exist in nucleolus as approximately 150 tandem-repeats in the wild-type. The size of one rDNA unit is ~9.1kb and the rDNA occupy 56% of chromosome XII. There are two ribosomal RNA genes, 35S rDNA and 5S rDNA in a unit. These genes are transcribed by RNA polymerase I (pol I) and III (pol III), respectively. The transcripts of 35S rDNA and 5S rDNA are pre-35S rRNA and 5S rRNA. The pre-35S rRNA is processed into matured 18S, 5.8S and 25S rRNAs. These rRNAs are essential components of ribosome. There are two inter genic spacers

(IGS1 and IGS2) that are located between 3'-35S rDNA and 3'-5S rDNA and between 5'-5S rDNA and 5'-35S rDNA, respectively. The replication fork barrier (RFB) and non-coding promoter (E-pro) are located in the IGS1. Cohesion associated region (CAR) and the replication origin (rARS) are located in the IGS2.

Because of repetitive structure of the rDNA, it easily forms the abnormal high-order structure that causes inhibition of DNA replication and induces DSB. In addition, DSB triggers the reduction of the copy number by popping out the copy and the recombination between the repeats. Consequently, the rDNA is known to be the most unstable region in the genome (Kobayashi, 2006). However, there is a system that maintains the rDNA stability, and each organism regulates the copy number at proper level. In the yeast *Saccharomyces cerevisiae*, a gene amplification system involving DNA recombination maintains the rDNA copy number (Kobayashi *et al.*, 1998) (Fig. 2). First, DSB occurs by the function of Fob1 at the RFB where inhibits the progression of replication fork in the rDNA. The DSB is induced on the leading strand of the fork (Burkhalter and Sogo, 2004). In case that this broken end is repaired with unequal sister-chromatid, some copies are replicated twice and the copy number increases (Kobayashi, 2006). This system amplifies the rDNA copy number at the rate of ~1 copy per cell division in the S phase of cell cycle. This process is induced when the copy number is reduced (Kobayashi *et al.*, 1998). Like this, rDNA copy is recovered by the DSB repair pathway with sister-chromatid recombination. However, once DSB recombines with improper copies,

deletional recombination of the repeats occurs, and the rDNA becomes unstable. Therefore, to avoid the risk, the rDNA is expected to have a system, recombination is properly regulated.

When DSBs by DNA damage is not repaired, checkpoint mechanism activates. The mechanism also activates in the rDNA, however, it occurs independently of homologous recombination (Mundbjerg *et al.*, 2015). Thus, I speculate that DSB in the rDNA is repaired immediately and restart of replication for the normal rDNA amplification. However, it is unclear the detailed mechanism how DSB in the rDNA is repaired.

In general, homologous recombination can randomly occur in the repeat sequences. Therefore, DSB in the rDNA should have a system to separate the broken ends to avoid such a random recombination with the other copies. In the previous study, it was shown that DSB induced artificially on the chromosome III physically interacted with components of the nuclear pore complex (NPC). This suggests that the nuclear pore is related to DSB repair in addition to the material transportation between nuclear and cytoplasm though the biological significance is unknown (Nagai *et al.*, 2008). I speculated that similar separation may occur in the rDNA and it functions to avoid improper recombination.

In our laboratory, by screening of genes that reduce rDNA stability, *TELI* was identified. *TELI* is an ortholog of ataxia telangiectasia mutated (ATM) in mammalian cells (Sabourin and Zakian, 2008). Ataxia telangiectasia (AT) is a multisystem syndrome that results from the mutation of *ATM*. In human, the patients have an increased risk for cancer and an

abnormal immune system (Economopoulou *et al.*, 2015). In budding yeast, *TEL1* plays an important role in telomere maintenance, especially in the replication of telomere (Shore and Bianchi, 2009). Tel1 protein is a member of Serine / Threonine kinase family. Through the kinase activity, telomerase elongates telomere (Shore and Bianchi, 2009). *TEL1* also participates in the checkpoint signaling response to DNA damage such as DSB (Longhese *et al.*, 2010). It plays an important role in the first step with *MEC1*. The checkpoint helps the cell to repair DSB. Although some functions of *TEL1* are known, it is still unclear why the rDNA is unstable by deletion of *TEL1*. Recently, the nuclear pore is remarked as repair scaffold and Tel1 is involved in the transport of unrepairable DSB to the NPC (Nagai *et al.*, 2008).

In this study, I tried to clarify whether DSB in the rDNA is located to the NPC. If it is the case, what kind of proteins participates in this process? First, in budding yeast, I analyzed the interaction between rDNA and nuclear pore complex by chromatin immunoprecipitation (ChIP) assay using anti-NPC antibody in the wild-type and the *fob1* mutant in which DSB in the rDNA doesn't occur. Next, I identified genes that are required for the localization of the rDNA to the NPC. Absence of Nup84, Arp5, and Mec1, the interaction between the rDNA and the NPC is decreased to compare with that of wild-type. These factors need for the anchoring of the HO-induced DSB to the NPC. Therefore, the rDNA is transported to the NPC by the similar pathway to the recruitment of the induced-HO DSB to the NPC. Moreover, I analyzed rDNA stability in these mutants by pulsed field electrophoresis (CHEF) and searched for genes directly

involved in the recruitment of DSB in the rDNA to the NPC. I identified the condensin recruiting factors as the transportation factors for the rDNA to the NPC.

I speculate that the NPC works as a transient anchoring scaffold to prevent DSB in the rDNA from recombining with the improper copies. In this study, together with the interaction between the rDNA and the NPC, I also investigated stability of the rDNA and found that the separation is required to rDNA maintenance. Moreover, I identified new factors for the separation of DSB in the rDNA that are not detected in the artificial system to induce DSB by HO endnuclease.

3. Results

3.1- Tel1 is involved in recombination repair for DSB caused by Fob1 at the RFB

TEL1 was identified through screening of genes that reduce rDNA stability. First we confirmed whether the phenotype is reproducible. To investigate the change of repeat number in the rDNA, chromosome XII (chr.XII) including rDNA, was analyzed by pulsed-field electrophoresis. Chr.XII was detected by southern hybridization with rDNA specific probe. In this analysis, we can judge the rDNA stability by the shape of the band. A sharp band indicates that the copy number doesn't change, that is, the rDNA is stable. On the other hand, a broader band indicates that the copy number frequently changes, that is, the rDNA is unstable. As the result, in the *tell* mutant, the rDNA was actually unstable to compare with that in the wild-type (Fig. 3). The band of the *fob1* mutant is sharper than that of the wild type, that is, rDNA is stable. This is because the replication fork is not arrested at the RFB and DSB to cause recombination is not induced (Kobayashi et al., 1998).

To uncover the function of Tel1 in the rDNA, I analyzed the relationship between Tel1 and Fob1. I investigated whether the rDNA instability in the *tell* mutant is Fob1-dependent or not. When *FOB1* was deleted in the *tell* mutant, the rDNA became stable (Fig. 3). Therefore, this suggests Tel1 functions in the downstream of Fob1 and it is involved in the recombination repair for DSB caused by Fob1 at the RFB.

Actually, *TEL1* maintains replication fork stability with *MEC1* (Doksani *et al.*, 2009).

We assumed that the reduced replication fork stability arrested at the RFB causes change of the repeat number in the rDNA in the *tel1* mutant. To test the possibility, we performed 2D-gel analysis. This analysis enables to separate replication and recombination intermediates according to these structures and observe DSB signal. In the *tel1* mutant, as the RFB signal is similar to that of the wild type, the fork stability should be fine. However, the DSB signal was weaker than that of wild-type (Fig. 4). In general, less DSB induces less instability. In contrast, as the rDNA is quite unstable in the *tel1* mutant, the broken end may be highly resected by abnormally repair and the amount of DSB was reduced.

3.2- The rDNA relocates to the NPC in a Fob1-dependent manner

Tel1 is required for the transportation of the HO-induced DSB to the NPC (Nagai *et al.*, 2008). Therefore, I speculated that naturally induced DSB in the rDNA is also transported to the NPC. To test the idea, I performed ChIP assay using anti-NPC antibody and investigated localization of the rDNA in wild-type. As a positive control, I used probes for telomere regions in chr. XII and chr. VI, because telomeres are known to be localized in the nuclear membrane (Palladino *et al.*, 1993; Gotta *et al.*, 1996). As a negative control, I also used probes in *CUP1* gene (data not shown).

For the ChIP assay I used four probes (RFB, 5S rDNA, 5'-35S rDNA, and 3'-35S

rDNA ; Fig. 5a, blue, red, green, purple). As the result, in the wild-type, the rDNA is surely located around the nuclear pore complex (Fig. 5b, c). Next, I performed ChIP assay using anti-NPC antibody in the *fob1* mutant. In contrast to the wild-type, interaction of the rDNA to the NPC was considerably decreased in all four regions in the rDNA (Fig. 5b, c).

To investigate whether the phenotypes in the *fob1* mutant depend on the *fob1* mutation, I performed a plasmid complementation experiment. The plasmid having the intact *FOBI* gene was transformed to the *fob1* mutant. The empty vector, not having the intact *FOBI* gene, was also transformed to the wild-type and *fob1* mutant. In the wild-type with the empty vector, the rDNA was transported to the NPC (Fig. 6a, b). When the intact *FOBI* gene is transformed in the *fob1* mutant, association between rDNA and NPC recovered (Fig. 6a, b). Therefore, the results confirm that the Fob1-dependent recruitment of rDNA to the NPC.

In addition, I performed ChIP assay in the *tell* mutant and found that NPC association with the rDNA was also clearly reduced in all four regions of the rDNA (Fig. 5b, c). Taken together, the rDNA is transported to the NPC in both Fob1- and Tel- dependent manners.

3.3- Factors for anchoring the HO – induced DSB to the NPC are also required for transportation of the rDNA to the NPC

In addition to Tell1, there are some factors that are involved in the transportation of the HO-induced DSB to the NPC and/or inner membrane protein Mps3 (Horigome *et al.*, 2014). To

identify genes that are required for localization of the rDNA to the NPC, I performed the ChIP assay in various mutants using anti-NPC antibody.

Nup84p is a subunit of the nuclear pore complex, forms the outer ring of nuclear pore (Strambio-De-Castillia C et al., 2010). The HO-induced DSB is known to be transported to the Nup84 complex (Nagai *et al.*, 2008). As the result of the ChIP assay using anti-NPC antibody, in the *nup84* mutant, the NPC association with the rDNA was also clearly reduced to compare with that in the wild-type (Fig. 7a, b).

I also investigated the nuclear pore association in a strain with Nup84 adding FLAG tag by ChIP assay using anti-FLAG antibody and compare with results of ChIP assay using anti-NPC antibody. The result of ChIP assay using anti-FLAG antibody was equivalent to that of ChIP assay using anti-NPC antibody (Fig. 8a, b). The association was also Fob1 dependent. These results indicate that the rDNA interacts with Nup84 of the NPC, and it is possible that the interaction is dependent on DSB at the RFB.

The INO80 and Arp5 are members of the chromatin remodeling complex that is conserved in eukaryotes (Yao *et al.*, 2015). This complex is involved in DNA repair and is recruited to the phosphorylated histone H2A (Morrison and Shen, 2009). Arp5, one of the actin-related proteins, also binds to DNA replication origins (Shimada *et al.*, 2008). Moreover, Arp5 is recruited to the HO-induced DSB by the accumulation of the phosphorylated histone H2A (van Attikum *et al.*, 2004). In the *arp5* mutant, the HO-induced DSB is transported to the

NPC (Horigome *et al.*, 2014). As the result of the ChIP assay using anti-NPC antibody, in the *arp5* mutant, the NPC association with the rDNA was clearly reduced to compare with that in the wild-type (Fig. 9a, b).

After the induction of DSB, yeast histone H2A around the DSB is phosphorylated (Shroff *et al.*, 2004). The phosphorylated histone H2A is called gamma-H2AX (γ -H2AX) in the yeast *S. cerevisiae* (Lee *et al.*, 2014). The serine of 129 (S129) of H2A is a target of phosphorylation by Mec1 and Tel1, DNA damage checkpoint kinases (Lee *et al.*, 2013). By altering the S129 of H2A to alanine, the *hta1S129A hta2S129A* mutant can be constructed. This mutant is not phosphorylated by Mec1 / Tel1. As the result of the ChIP assay using anti-NPC antibody, in the *hta1S129A hta2S129A* non-phosphorylated mutant, the NPC association with the rDNA was reduced to compare with that of the wild-type (Fig. 10a, b).

Mec1 (ortholog of human ATR) is one of the DNA damage checkpoint kinases, and has an important role for DNA damage check-point activation (Friedel *et al.*, 2009). Mec1 and Tel1 catalyze the phosphorylation of Rad53 (Pelliccioli and Foiani, 2005). Mec1 also phosphorylates histone H2A with Tel1 in response to DNA damage (Lee *et al.*, 2013). In *S. cerevisiae*, *MEC1* is an essential gene. However, the lethality is suppressed by deletion of the ribonucleotide reductase inhibitor Sml1 (Zhao *et al.*, 2000). Therefore, I performed ChIP assay in the *sml1 mec1* double mutant. As the result of the ChIP assay using anti-NPC antibody, in the *sml1 mec1*

mutant, the NPC association with the rDNA was reduced to compare with that of the wild-type (Fig. 11a, b).

Sir2 is conserved well in eukaryotes and is known to one of long-life associated genes. In the yeast *S. cerevisiae*, the *sir2* mutant has shorter lifespan than the wild-type. Sir2 functions as a histone deacetylase (HDAC) that is responsible for gene silencing in telomere, rDNA and silent mating type loci (Cuperus *et al.*, 2000). Moreover, in the rDNA, Sir2 plays an important role in maintenance of sister chromatid cohesion to reduce the frequency of unequal sister chromatid cohesion (Kobayashi *et al.*, 2004). Although the rDNA is unstable in the *sir2* mutant, as the result of the ChIP assay using anti-NPC antibody, the rDNA association with the NPC is similar to that of wild-type (Fig. 12a, b). Therefore, Sir2, a key factor in rDNA amplification recombination, is not involved in the recruitment system.

In the *nup84* (Fig. 7), *arp5* (Fig. 9), *hta1S129A hta2S129A* (Fig. 10), and *mec1* mutants (Fig. 11), the rDNA association with the NPC was clearly reduced to compare with the wild-type. On the other hand, in the *sir2* mutant (Fig. 12), the rDNA association with the NPC was similar to that of the wild-type. Consequently, some factors involved in the transportation of the HO-induced DSB to the NPC and/or Mps3 were also related to the transportation of the rDNA to the NPC.

3.4- Condensin recruiting factors to the RFB are required for the transportation of the

rDNA to the NPC

As DSB is naturally induced in the rDNA, I speculate there are specific factors required for this recruitment pathway to the NPC. I focused on proteins that present and function in both rDNA and nuclear membrane. Tof2, Csm1 and Lrs4 actually present in the both regions. They are related to condensin recruitment to the RFB site (Johzuka and Horiuchi, 2009). Tof2 binds to Fob1, Csm1 and Lrs4 complex interact with this Tof2, and then condensin is recruited to the RFB. By the recruitment, the rDNA is condensed and the chromosome can segregate properly. These three factors, especially, Csm1 and Lrs4 are also known to present on the nuclear membrane (Huang *et al.*, 2006) and the association is important for rDNA stability (Mekhail *et al.*, 2008). I performed ChIP assay using anti-NPC antibody in the *tof2*, *csm1* and *lrs4* mutant. In these mutants, rDNA association with the nuclear pore complex was also clearly reduced to compare with that in the wild-type (Fig. 13a, b). Therefore, these results indicate that the condensin recruitment factors are also involved in the localization of DSB in the rDNA to the NPC.

3.5- The transportation of the rDNA to the NPC affects rDNA stability

In the HO-induced DSB experiment, the homologous sequences for the DSB repair are deleted and the experiment is performed in the G1 phase of cell cycle (Nagai *et al.*, 2008). Therefore, the DSB repair process is not observed. On the other hand, in case of the rDNA, the

DSB is repaired by usual homologous recombination with the sister-chromatid or other copies. To test the effect of recruitment for the repair, I investigated rDNA stabilities in the mutants that have reduced interactions with the nuclear pore complex by pulsed field gel electrophoresis. The results are shown in Fig.14. As the control, I tested *fob1* (Kobayashi et al, 1998) and *sir2* mutants (Kobayashi *et al.*, 2004). In the *fob1* mutant the band of chr.XII is sharper and in the *sir2* mutant the band is broader than that in the wild type. These indicate that the rDNA is more stable and less stable to compare with the wild type, respectively. In the *csml* and *lrs4* mutants, the rDNA was less stable to compare with that in the wild-type as reported (Mekhail *et al.*, 2008). In the *hta1S129A hta2S129A*, *mec1*, *tof2* and *lrs4* mutants, the rDNA was also less stable to compare with that in the wild-type (Fig. 14a, b). Moreover, in the *nup84*, *arp5* and *csml* mutants, the rDNA was slightly unstable though the chromosome is duplicated in the *arp5* mutant. Taken together, these suggest that the localization of DSB in the rDNA to the NPC affects rDNA stability.

3.6- A histone variant is not involved in the transportation of the rDNA to the NPC

Htz1 is a variant of histone H2A in the yeast *S. cerevisiae* (Jackson and Gorovsky, 2000). As DSB is induced in a DNA region, the histone H2A of the DSB site replaces the histone variant Htz1 (van Attikum *et al.*, 2007). Incorporation of Htz1 to the nucleosome in the DSB site is mediated by the chromatin remodeling complex SWR1 (Luk *et al.*, 2010, Mizuguchi *et al.*,

2004). Reversely, the incorporated Htz1 is eliminated by INO80 complex from the DSB site (Papamichos-Chronakis *et al.*, 2006). In the *swr1* and *htz1* mutants, the HO-induced DSB is not transported to the NPC (Horigome *et al.*, 2014).

To investigate whether Htz1 is required for the transportation of the rDNA to the NPC, I performed ChIP assay using anti-NPC antibody in the mutant. As the result, in the *htz1* mutant, the rDNA association with the NPC is similar to that of wild-type (Fig. 15a, b). Therefore, I concluded that Htz1 is not involved in the transportation system of the rDNA to the NPC.

3.7- Ubiquitin ligases are related to the transportation of rDNA to the NPC

In the pathway of unreparable DSB to the NPC, Slx5 and Slx8, members of SUMO-targeted ubiquitin ligases (STUbLs) have an important role for genome stability (Nagai *et al.*, 2011). The STUbLs family is conserved from yeast to mammal and SUMO proteins are enriched at the NPC. These proteins associate with the DSB and the broken end is recruited to the NPC. In addition, SUMO proteins are also involved in the maintenance of rDNA stability by reducing recombination with improper copies (Torres-Rosell J *et al.*, 2007).

To investigate whether ubiquitin ligases are required for the transportation of rDNA, I performed ChIP assay using anti-NPC antibody in the *slx5* and *slx8* mutants. As the result, in the *slx5* and *slx8* mutants, the rDNA association with the NPC is slightly decreased to compare with that of wild-type (Fig. 15a, b). Therefore, contribution of SUMO proteins to the transportation of

rDNA to the NPC might be minor.

3.8- The rDNA is transported not only to the NPC but also to Mps3

Mps3 is the inner membrane protein that is required for the recruitment of the HO-induced DSB to the nuclear membrane (Oza *et al.*, 2009). In *S.cerevisiae*, Mps3 is an essential protein (Jaspersen *et al.*, 2002) for establishment of Spindle Pole Body (SPB) that corresponds to the Centriol in mammal (Nishikawa *et al.*, 2003). Moreover, Mps3 is required for localization of telomere with nuclear membrane (Antoniacci *et al.*, 2007; Bupp *et al.*, 2007).

To test whether Mps3 is required for the transportation of rDNA to the NPC, I performed ChIP assay using anti-NPC antibody in the *mps3* mutant. In this mutant, only N-terminal acidic domain of Mps3 is deleted to maintain viability of the cell. This *mps3* mutation declines telomere localization on the nuclear membrane in S phase but maintains the distribution of nuclear pore on the nuclear membrane (Oza *et al.*, 2009). As the result of the ChIP assay using anti-NPC antibody, in the *mps3* mutant, the NPC association with the rDNA was similar to that of the wild-type (Fig. 16a, b).

Then, I performed ChIP assay in the *fob1* mutant with Mps3-FLAG using anti-FLAG antibody and compare with results of ChIP assay using anti-NPC antibody. As the result, the association of the rDNA with Mps3 is reduced as in the *fob1* mutant (Fig. 17a, b). Therefore, the rDNA is recruited to Mps3 in a Fob1 dependent manner, too.

3.9- The RFB is not always required for the transportation

Tof1 is a subunit of the replication-pausing checkpoint complex (Tof1-Mrc1-Csm3), and Rrm3 is a helicase in the rDNA replication. Tof1p is required to maintain the fork stability and also fork arrest at the RFB. In the 2D gel analysis, the RFB spots in wild-type are almost abolished in the *tof1* mutant (Bastia *et al.*, 2006). In addition, in the *tof1* mutant, the rDNA is unstable (Saka *et al.*, submitted). On the other hand, in the absence of the Rrm3p helicase, there was a slight enhancement of replication fork arrest at the RFB sites in comparison with the wild-type (Bastia *et al.*, 2006). As these mutants affect on the fork block activity, we investigated the recruitment of the rDNA to the NPC by CHIP assay in these mutants. As the result of the CHIP assay using anti-NPC antibody, both in the *tof1* and *rrm3* mutants, the rDNA association with the NPC is similar to that of wild-type (Fig.16a, b). As DSB is expected to be occurred in the *tof1* mutant, the RFB is not always required for the transportation to the NPC. In this case, the transportation may be similar to the HO-induced one.

4. Discussion

In this study, I found the rDNA is transported to the NPC and Mps3 in *S. cerevisiae*. As the rDNA is spontaneously and highly recombinogenic region, this transportation should have important physiological functions to maintain rDNA stability. Actually, mutation in the pathway reduced rDNA stability. The results in this study suggest that DSB in the rDNA is repaired at the nuclear pore complex. In addition, I identified that Tel1 and some other genes are required for the recruitment of DSB in the rDNA to nuclear pore complex. In HU-treated cells, Ino80 is recruited to the RFB site in the rDNA (Shimada *et al.*, 2008). However, it was unclear whether Tel1 and some other genes are actually recruited to the rDNA region. Some condensin recruitment genes are included in the genes for transportation of rDNA. In addition, for the transportation to the NPC, the inner membrane protein, Mps3 wasn't required, however, the rDNA is also associated to Mps3 in a Fob1-dependent manner. As the conclusion, I will present a model as follow.

DSB is induced at the RFB site in the rDNA by the function of Fob1. Mec1/Tel1 phosphorylated histone H2A of the DSB and Ino80 complex is recruited to the phosphorylated histone H2A. Then the rDNA is transported to the NPC and/or Mps3 (Fig. 18). I assume that the condensin recruiting factors might transport the rDNA to the NPC and/or Mps3. This transportation system prevents DSB from recombining with improper copies and ensures the

normal chromosome segregation. Therefore, I assume that this transportation system maintains rDNA stability and regulates the senescence of mother cell.

4.1- rDNA association to the NPC

I performed ChIP assay to investigate the localization of DSB in the rDNA. As the result, DSB in the rDNA is surely associated with the nuclear pore complex. It is better that this phenomenon is confirmed by other methods except ChIP assay, for example, with microscopy. Actually, the transportation of HO-induced DSB was observed by microscopy (Nagai *et al.*, 2008). Moreover, an I-SceI-induced DSB in the rDNA relocates to the extranucleolar site for repair (Torres-Rosell *et al.*, 2007). While, it is known that the rDNA repeat presents in the nucleolus through the cell cycle (Miyazaki and Kobayashi, 2011). In the wild-type, the rDNA copy number is about 150. Among them, only a few copies are broken (Zou and Rothstein, Cell). I speculate Therefore, it could be difficult to observe the direct interaction between DSB in the rDNA and the nuclear pore because most of rDNA copy is still located in the nucleolus.

I performed ChIP assay by using anti-Nuclear Pore Complex Proteins antibody. This antibody recognizes the proteins in the NPC that contain phenylalanine-glycine (FG) repeats. NPC proteins containing this repeats are especially called FG Nups and are well conserved through species. As the NPC is a huge protein complex, the antibody precipitates the whole complex with the associating DNA. However, as in the *nup84* mutant the rDNA association to

the NPC was much reduced, Nup84 is mainly associated with rDNA.

As for unreparable HO-induced DSB, DSB association with nuclear pore complex is observed even 9.6kb away from the HO cut site (Nagai *et al.*, 2008). As a unit of rDNA is about 9.1kb (Kobayashi, 2006; Miyazaki and Kobayashi, 2011), it is not so surprising that all over the rDNA region is associated with the nuclear pore complex. Therefore, I speculate that DSB specifically associates with Nup84 and other part of rDNA may non-specifically interact with other components of NPC.

4.2- What is the role of Tel1 in rDNA stability rDNA?

This study uncovered that Tel1 is required for the transportation of the rDNA to the NPC. In addition, the CHIP assay using anti-NPC antibody uncovered that the phosphorylated histone H2A is also involved in the transportation. Therefore, these suggest that Tel1 functions to phosphorylate the histone H2A of DSB in the rDNA. In mammalian cells, the phosphorylated histone H2AX (γ -H2AX) is a specific DSB marker (Turinetto and Giachino, 2015). In the yeast *S. cerevisiae*, throughout about 5kb around a break site, γ -H2A is formed (Shroff *et al.*, 2004). In case that Tel1 is not functioning, the rDNA is not transported to the NPC and DSB in the rDNA might be not repaired correctly. Therefore, the phosphorylated histone H2A by Mec1/Tel1 is possibly the trigger of the transportation of the rDNA to the NPC.

Tel1 maintains replication fork stability with Mec1 (Doksani *et al.*, 2009; Lopes *et al.*,

2001). In addition, Mec1 and Tel1 prevent the fork collapse (Branzei and Foiani, 2010). As in the *mec1* and *tel1* mutants, the interaction between the rDNA and the NPC is decreased compare to that of wild-type, I first assumed that the fork collapse causes change of the repeat number in the rDNA in these mutants. However, in Fig.4, as the RFB signal was not reduced in the *tel1* mutant, the fork at the RFB is not collapsed. Therefore, the *tel1* mutation doesn't affect the fork stability. Instead, the mutation may reduce recombination repair after DSB.

In mammalian cells, DSB in the nucleolus causes ATM-dependent silencing of the transcription by RNA polymerase I (Pol I) (Kruhlak *et al.*, 2007). In addition, by ATM-dependent silencing of the rDNA transcription, DSB in the rDNA is located at the nucleolar periphery, and is recognized by DNA damage response factors (Harding *et al.*, 2015). If Tel1 dysfunctions on the rDNA in *S. cerevisiae*, DSB in the rDNA might be not recognized by DNA damage response factors and it might be not repaired correctly. As the result, the broken end is recombined with improper copies. I assume Tel1 acts on the transportation of the rDNA to the NPC and the relocation is required for the proper repair.

4.3- Is the interaction actually dependent on DSB in the rDNA?

I showed that the rDNA interaction with NPC is “*FOBI*” dependent. However, there is no evidence that the interaction is “DSB” dependent. I speculate that rDNA behaves as the HO-induced DSB dose. It is possible that the arrested fork by the function of Fob1 or Fob1

association to the RFB itself is necessary for the transportation. As the result of the ChIP assay using anti-NPC antibody in the *tof1* mutant and the *rrm3* mutant, the rDNA association with the NPC was similar to that of wild-type (Fig.16). If stalled fork is transported to the NPC, the rDNA association with the NPC should decrease in the *tof1* mutant and increase in the *rrm3* mutant compare to that of wild-type. As well as Rrm3, the Pif1 helicase is associated with rDNA, has an important role for rDNA replication (Ivessa *et al.*, 2000). In the *pif1* mutant, rDNA breakage and level of rDNA circles decreased compare to that of wild-type. To check the involvement of Pif1 to the transportation, we need to perform the ChIP assay in the *pif1* mutant. In addition, Tof1 is required for fork-stabilizing (Voineagu *et al.*, 2008). The replication fork destabilizes in the *tof1* mutant, and DSB is most likely induced in the region except the RFB. Therefore, we need to perform the 2D gel analysis in the *tof1* mutant, and investigate the signal pattern. Moreover, to investigate whether DSB increases and the rDNA is transported to the NPC, we need to perform the ChIP assay in the *fob1 tof1* double mutant.

4.4- Why is rDNA not so unstable in the transportation-related factors mutants?

As the result of CHEF and the southern hybridization, in the *hta1S129A hta2S129A*, *tell*, and *mec1* mutants, the rDNA was much less stable to compare with that in the wild-type (Fig. 14). Moreover, in the *nup84* mutant, the rDNA was slightly unstable. One possible idea is that the relocation itself is not related to the DSB repair. On the way to the NPC, most of DSB is

repaired. For example, in the *nup84* mutant, rDNA is not relocated to the NPC. But the Tel1-dependent transportation is induced and the DSB is repaired outside of the nucleolus with proper sister chromatid. Therefore, rDNA is not so unstable. During the repair process, a very few DSB is not repaired properly and relocated at the NPC in a Nup84 dependent manner. In other words, in the *tell* mutant, as neither repair nor translocation occurs, the rDNA becomes unstable. On the contrary, in the *nup84* mutant, as repair occurs but relocation doesn't occur, the rDNA is less unstable. In fact, the HO-induced DSB is unreparable and relocated to the NPC (Nagai *et al.*, 2008). I assume the transportation of DSB to NPC is the system for isolation of the unrepaired DSB from other DNA to avoid recombination with improper copies.

4.5- Is condensin involved in the transportation of the rDNA to the NPC?

Condensin regulates the rDNA compaction. In addition, condensin is important for DSB repair and the mutants are sensitive to the UV (Sheedy *et al.*, 2005). Condensin is thought to promote the equal sister-chromatid recombination by attachment of sister-chromatids (Ide *et al.*, 2010). This study indicates that condensin recruiting factors to the RFB are involved in the transportation of the rDNA to the NPC. Therefore, condensin is also possibly involved in the transportation. I assume that condensin recruiting factors act as the transporter of the rDNA to the NPC, and condensin condenses the rDNA around the NPC to facilitate the chromosome segregation. To investigate the direct involvement of condensin to the transportation, we need to

perform the ChIP assay in the condensin mutant.

4.6- Dynamics of the rDNA in the nucleolus with regards to this transportation system

The condensin recruiting factors, Csm1 and Lrs4 (Mekhail *et al.*, 2008) interact with the CLIP (chromosome linkage INM protein) complex that anchor the rDNA to the nuclear envelope to stay the rDNA in the nucleolus. The complex keeps the rDNA away from DNA recombinases (Rad52 etc) in the nucleoplasm and maintains rDNA stability (Mekhail and Moazed, 2010). In general, the rDNA exists in the nucleolus throughout cell cycle (Miyazaki and Kobayashi, 2011) in which there isn't DNA repair factor in the nucleolus (Torres-Rosell *et al.*, 2007). Therefore, the rDNA has to go out the nucleolus for repair. Actually, in the *rad52* mutant, the rDNA copy number did not recover in the strain having approximately 80-copies (Kobayashi *et al.*, 2004).

This study suggests ubiquitin ligases are involved in the transportation of the rDNA to the NPC though the contribution is minor. In the *slx5* mutant, and especially in the *slx8* mutant, the rDNA association with the NPC was a little decreased to compare with that of wild-type (Fig. 15). Slx5 and Slx8 have a key role for genome stability (Zhang *et al.*, 2006). They are a heterodimeric complex in the yeast *S. cerevisiae* (Cook *et al.*, 2009), The Slx5-Slx8 complex reflects on the sumoylation of DNA repair factors containing Rad52 (Burgess *et al.*, 2007). In addition, in the *slx8* mutant, the rDNA recombination is increased in a Rad52 dependent manner (Eckert-Boulet and Lisby, 2009). The frequency of nucleolar Rad52 foci is also increased in the

slx8 mutant (Burgess *et al.*, 2007). Therefore, the Slx5-Slx8 complex has a role for the regulation of the rDNA recombination. As for the transportation of the rDNA to the NPC, the complex is not so critical.

4.7- What is the role of Mps3 in the transportation of the rDNA to the NPC?

In the yeast *S. cerevisiae*, Mps3 has a role for establishment of spindle pole body (SPB) (Jaspersen *et al.*, 2002). The HO-induced DSB is transported to Mps3 in an INO80 complex dependent manner (Oza *et al.*, 2009 and Horigome *et al.*, 2014). My results suggest that the transportation of the rDNA to the NPC possibly requires INO80 complex. In this study, I did not perform the ChIP assay in the *ino80* mutant (non-essential gene). One of the subunit of INO80 complex, Ino80 has a role as ATPase for chromatin remodeling (Seeber *et al.*, 2013). Actin-related proteins, such Arp5 and Arp8, are required not only for the recruitment of INO80 complex to chromatin but also for the ATPase activity of INO80 complex (Osakabe *et al.*, 2014). In addition, in the *htz1* mutant, the rDNA association with the NPC was similar to that of wild-type (Fig. 15). Htz1 is necessary for the transportation of the HO-induced DSB to Mps3 (Horigome *et al.*, 2014). Therefore, the incorporation of Htz1 by SWR1 chromatin remodeling complex is possibly required for the transportation of the rDNA to Mps3, not to the NPC.

SPB and NPC link on the nuclear envelope (Jaspersen and Ghosh, 2012). The SPB is important for chromosome segregation. Centromeres of chromosomes are tethered to the SPB

(Taddei *et al.*, 2010). This tethering permits to segregate chromosomes. My results indicate that the transportation of the rDNA to the NPC requires condensin recruiting factors. Consequently, by the cooperation of Mps3 and condensin recruiters, the rDNA is normally condensed and chromosome might be easy to segregate.

4.8- Association of the transportation of the rDNA to the NPC for aging

After the induction of unrepairable DSB, it takes for 2~4h to transport the DSB to the NPC (Nagai *et al.*, 2008). On the other hand, DSB in the rDNA could occur frequently by blocking replication fork at the RFBs, and the broken end is quickly repaired in one way or another. In this study, I identified genes that are involved in the recruitment of the rDNA to the NPC. However, it is unclear when and which these factors act on the recruitment pathway. Moreover, although there are approximately 200 NPCs on the nuclear membrane in the yeast *S.cerevisiae*, it is unknown which NPCs on the nuclear membrane interacts with the rDNA.

The condition of rDNA (the copy number and stability) affects the function of the cell. Notably, it is known that cellular senescence (replicative senescence) is affected by rDNA stability (Kobayashi, 2008). In the budding yeast *S. cerevisiae*, whenever a cell (mother cell) produces a new cell (daughter cell), the mother cell becomes older, and dies finally. On the other hand, the newborn daughter cell doesn't inherit the aging phenotypes of the mother cell and achieves the rejuvenation. To rejuvenate the daughter cell in the cell division, the mechanism of

the mother cell aging is uncovering. The previous study proposes the hypothesis that the instability of the rDNA is a cause of the aging (Kobayashi, 2006). In this hypothesis, according to cell divisions, the mother cell specific rDNA instability is induced (Ganley *et al.*, 2009). However, the mechanism to distinguish between the mother cell and the daughter cell is still unknown. In this current study, it uncovers that condensin recruiting factors needs for the transportation of the rDNA to the NPC. Condensin functions the unity of the rDNA. Dysfunction of condensin causes non-disjunction of chromosomes. Therefore, I speculate that the unequal distribution of the rDNA between mother cell and daughter cell contributes to the differentiation of both cells and the transportation links the rDNA stability and aging. I expect that the NPC and condensin become a key to solve the cooperation between these mechanisms.

5. Acknowledgements

I'm grateful thank to Prof. Takehiko Kobayashi for constant guidance during my PhD study. I thank Dr. Kenji Shimada (Friedrich Miescher Institute for Biomedical Research), Prof. Masahiko Harata (Tohoku University), Prof. Masato Kanemaki, and Assistant Prof. Chihiro Horigome for providing us various yeast strains and plasmids in this study. I also thank Prof. Hiroyuki Araki, Assistant Prof. Chihiro Horigome and Assistant Prof. Mariko Sasaki for advice and discussion throughout my study. Moreover, I appreciate to Assistant Prof. Tetsushi Iida, Assistant Prof. Yuhuko Akamatsu, Kimiko Saka, and the all progress committee members for supporting my PhD study.

6. Material and Methods

Yeast strains, plasmids, and growth conditions

Yeast strains used in this study were derived from NOY408-1b (W303 derivative). Unless indicated, strains were grown at 30 ° C in YPD medium. YPD (yeast extract-peptone-dextrose) is rich medium for the normal culture, YP-Galactose (yeast extract-peptone-galactose) is for induction of *GAL* promoter and synthetic complete (SC) medium lacking the appropriate amino acids (Sherman *et al.*, 1986) is for the gene maker selection. To control the *FOBI* expression under the *GAL7* promoter, cells were pre-cultured in medium containing 2% (w/v) raffinose as a sole carbon source until induction. Induction of *FOBI* was triggered by adding galactose solution to the culture (2% [w/v].) Plasmids were maintained in *Escherichia coli* DH5 α strain. Yeast strains and plasmids used in this study are listed in Table 1, 2.

Medium used for yeast cell culture is listed in Table 3. They were prepared as described (Dan Burke, 2000) with some modification. If necessary, G418 (Sigma) and 5-Fluoroorotic acid (5-FOA; Wako) were added to the medium with the concentration shown in Table 3.

PCR primers

PCR primers used in this study are listed in Table 4. Primers were stored in 50 μ l TE

buffer at -20 °C freezer.

Yeast genetic transformation

Yeast genetic transformation was performed by using Frozen-EZ Yeast Transformation II Kit (Zymo Research Corporation) according to the instruction of manufacturer. Yeast cells were cultured in appropriate liquid medium (10ml) until mid-log phase (O.D. ~1.0, 600nm) and collected by centrifugation at 10,000 rpm for 1 min. Cells were washed with 0.5 ml of EZ solution 1 and repelleted. After supernatant was discarded, $\sim 1 \times$ cells were suspended into 50 $\mu\ell$ of EZ solution 2 for one transformation reaction. 5 $\mu\ell$ of DNA solution (~ 200 ng/ $\mu\ell$) was mixed with the cell suspension, 500 $\mu\ell$ of EZ solution 3 was added and suspended gently. The mixture was incubated in 30 °C for at least 45 min with vigorously mixing every 15 min. Cell mixture was pelleted by centrifugation at 10,000 rpm for 1 min, and spread onto an appropriate plate medium. When a drug resistance marker was used for selection, cells were cultured in non-selective liquid medium for at least 2 h before spreading.

Plasmid construction

The galactose-inducible *FOBI* plasmid, YCplac33-*GALFOBI*, was constructed as follow. ~ 3 kb fragment that contains galactose-inducible *FOBI* cassette was excised from YCp*GALFOBI* by BamH I / Sal I digestion and sub-cloned into these sites of YCplac33.

DNA labeling with radioactive dCTP

Radio labeled DNA probes for Southern hybridization was obtained as follow. To label DNA fragments with [α -] dCTP, High Prime (Roche diagnostic) was used according to the instruction of manufacturer. Before the labeling, the template DNA (probe, 50 ng) in dH₂O was boiled for 10 min and immediately chilled on ice. The template DNA was mixed and 5 μ l of [α -] dCTP, then incubated for at least 10 min at 37 ° C for labeling. After the reaction was finished, labeled DNA was purified by using NICK columns (GE). For denaturing, the purified DNA was boiled for 5 min, immediately chilled on ice for at least 1 min and then used for hybridization.

Southern blotting and hybridization

DNA transfer from agarose gel to nylon membrane was performed as described previously (Sambrook and Russell, 2001). After electrophoresis, the DNA was depurinated in 0.2 N HCl, denatured in Denaturation buffer (see Table 5), and neutralized in Neutralization buffer (see Table 5) for 20 minutes, respectively. Next, the DNA was transferred to Nylon membrane (Hybond N+ , GE) in 20 \times SSC by capillary transfer for at least 15 h. After the membrane was washed with 6 \times SSC, DNA was cross-linked to the membrane before the hybridization with 120 mJ of UV (254 nm) irradiation by Stratalinker (Stratagene).

The membrane was pre-hybridized in 40 ml Hybridization buffer (see Table 5) at 65 ° C for 30 min, followed by hybridization in 40 ml of Hybridization buffer containing heat-denatured

probe at 65 °C for overnight in a roller bottle. The membrane was washed with 2 × SSC, 2% SDS for 30 min at 65 °C and in 0.2 × SSC, 0.2% SDS for 30 min at 65 °C. Next, the membrane was briefly rinsed with 0.2 × SSC, 0.2% SDS at room temperature. Then, the membrane was exposed to the Imaging plate (GE) for a day. The signals were detected by Typhoon FLA 9000 (GE) and analyzed by Image Quant (GE).

Pulsed field (CHEF: Countour- clamped homogenous electric field) electrophoresis

Samples for pulsed-field (CHEF) electrophoresis were prepared as described previously (Kobayashi *et al.*, 2001) using ~1.0× cells per one plug. The sample plug was cut in half and used for electrophoresis.

Electrophoresis was performed in a 0.8% agarose gel with 0.5 × Tris-borate-EDTA (TBE) buffer, using CHEF-MAPPER (Bio-Rad). For Fig. 1, the conditions were a 300-900 sec pulse time and 100V for 68 hours at 14 °C in a 0.8% agarose gel.

Two-dimensional (2D) gel electrophoresis

To detect replication and recombination intermediates and DSB spot by 2D gel electrophoresis (Ide and Kobayashi, 2010), DNA was prepared from cells growing in YPD, and DNA was isolated and embedded in plugs (Ide *et al.*, 2010). Yeast cells were cultured in YPD medium until mid-log phase (O.D. 0.8, 600nm). After the incubation on ice, 10% sodium azide

(final conc. 0.1%) was added to the sample. The sample cells were collected by centrifugation at 3,500 rpm for 5 min at 4 ° C. After supernatant was discarded, the cells were suspended into 10 ml ice-cold sorbitol solution with sodium azide for cell wash. The cells were collected by centrifugation at 3,500 rpm for 5 min at 4 ° C, then supernatant was discarded. This sorbitol solution with sodium azide wash was performed twice. There are $\sim 1.0 \times$ cells in each plug.

i) Digestion with restriction enzyme

The plugs were treated with Bgl II . Before the digestion of the restriction enzyme, the plugs were put in 1.5 ml tubes, 1 ml TE buffer (pH 8.0) was added to the tubes for wash. After the incubation for 30 min at room temperature, supernatant was discarded. This incubation was performed twice. After that, 0.5 ml $1 \times$ reaction buffer was added to the tube. After the incubation for 30 min at room temperature, the buffer was discarded. This incubation was performed twice. DNA in the plugs were digested with Bgl II for 4h at 37 ° C. The reaction was carried out in 200 $\mu\ell$ $1 \times$ reaction buffer with 150 units of Bgl II .

ii) The first dimension gel electrophoresis

The plugs were set in 0.4% agarose gel (200 ml $1 \times$ TBE, 0.8g SeeKem LE agarose), the first dimension electrophoresis was performed at 32V/cm for 12~13h at room temperature. After the electrophoresis, the gel was stained in 300 ml $1 \times$ TBE containing 0.5 μ g/ml ethidium bromide for 30 min at room temperature. After the staining, the electrophoresis band patterns were checked. By this first dimension electrophoresis, DNA in the plugs was separated with size.

iii) The second dimension electrophoresis

The gel (lane) containing the objective size was excised from the first dimension gel, turned it 90°, and put on the second dimension gel tray. 1.2 % agarose solution (200 ml 1 × TBE, 2.4g SeeKem LE agarose, 6.0 μl 10mg/ml ethidium bromide at ~55 °C) was poured to the tray, and the gel was hardened for 20min at room temperature. The second dimension electrophoresis was performed at 132V/cm for 4.5h at 4 °C.

iv) Signal detection

After the check of the electrophoresis band patterns, the DNA was transferred to the membrane. The membrane-bound DNA was hybridized with a radiolabeled probe. The rDNA was detected with an rDNA specific probe. After wash, the membrane was exposed to the Imaging plate (GE) for a week. The signal was detected by Typhoon FLA 9000 (GE) and were analyzed by Image Quant (GE).

DNA sequencing

DNA sequencing was performed by using BigDye® Terminator v3.1 Cycle Sequencing Kits (Applied Biosystems) and 3130xl Genetic Analyzer (Applied Biosystems) according to the instruction of manufacturer.

Western blotting

Yeast whole cell extracts were prepared by the TCA method (Ide *et al.*, 2010). Proteins were fractionated by SDS-polyacrylamide gel electrophoresis (PAGE), transferred to a PVDF membrane (Millipore) and subjected to Western blotting analysis as described previously (Ide *et al.*, 2010). For detection of a related family of nuclear pore complex (NPC) proteins, anti-nuclear pore complex proteins antibody Mab414 (Abcam) or anti-FLAG antibody, F2 were used.

Chromatin immunoprecipitation

ChIP analysis was performed based on the method described previously (Aparicio *et al.*, 2004). Buffers used in this assay are shown in Table 5. Yeast cells were cultured in appropriate liquid medium until mid-log phase (O.D. 0.6~0.8, 600nm).

i) Cross-link protein-DNA complexes *in vivo*

Cells were fixed in 0.55ml 37% formaldehyde for 20 min. After that, 3ml 2.5M Glycine was added to stop the cross-link reaction for 5 min. The cells were collected by centrifugation at 3500 rpm for 3 min at 4 °C. After supernatant was discarded, the cells were suspended into 5ml of ice-cold TBS (see Table 5) solution for cell wash. The sample cells were collected by centrifugation at 3,500 rpm for 3 min at 4 °C, then the supernatant was discarded. This TBS wash was performed twice. Next, the cells were suspended into 5ml of ice-cold FA lysis buffer (see Table 5) for cell wash. The cells were collected by centrifugation at 3,500 rpm for 3 min at 4 °C, then the supernatant was discarded. This FA lysis buffer wash was performed three times.

ii) Lyse cells and isolate chromatin

After cell wash, the sample cells were suspended into 0.5ml of ice-cold FA lysis buffer / 2mM PMSF. These samples were transferred to 2.0ml screw cap microfuge tubes (Sarstedt). This tube was pre-added 1.7g Glass beads, acid washed 425-600um (SIGMA). These tubes were closed by screw caps tightly, and mixed by inversion. By using Multi-Beads Shocker (YASUI KIKAI), the beads in the tubes were stirred and the cells were crashed in the condition (interval [ON 30 sec: OFF 60 sec] × 16).

iii) Isolate lysate

The bottom of the tube was punched a hole by a needle and the tube was inserted to a size larger tube. The samples were collected by centrifugation at 3,500 rpm for 3 min at 4 °C. The collected sample was transferred to a 1.5ml Eppendorf tube. The sample was collected by centrifugation at 15,000 rpm for 15 min at 4 °C, then the supernatant was discarded.

iv) Shear DNA

The samples were suspended into 0.5ml of ice-cold FA lysis buffer. The suspension sample was transferred to the tubes for sonication by Bioruptor (Cosmo Bio). The tube was set to the machine, and DNA sheared in the condition (interval [ON 30sec: OFF 30sec] × 9) to reduce the average size of DNA fragment to ~500bp. The sonicated samples were transferred to new eppendorf tubes, and collected by centrifugation at 15,000 rpm for 30 min at 4 °C. The supernatants were transferred to new eppendorf tubes, stored -80 °C deep freezer. This was used

as the whole cell extract (WCE) for ChIP assay.

v) Check chromatin fragment size

50 $\mu\ell$ WCE was added 50 $\mu\ell$ ChIP elution buffer (see Table 5). Next, 4 $\mu\ell$ 20mg/ml proteinase K (Merck) in PBS was added to the 100 $\mu\ell$ sample, and it was incubated for 2h at 37^o C and for 6h at 65^o C. Proteins were removed by phenol chloroform, and DNA was precipitated by ethanol. After 70% ethanol wash, dried fragments were suspended into 4 $\mu\ell$ TE buffer (pH 8.0). The 2 $\mu\ell$ suspension was added 1 $\mu\ell$ dH₂O and 1 $\mu\ell$ 10 \times loading buffer (TaKaRa). These samples were applied to 1.5% agarose gel, and performed electrophoresis with 100bp DNA ladder marker (New England Biolabs, NEB) for 18min at 135V.

vi) Immunoprecipitate

1 $\mu\ell$ anti-nuclear pore complex (NPC) protein antibody (Mab414, abcam) (1,000mg/ml) was suspended to 10 $\mu\ell$ Dynabeads Protein G . Total 11 $\mu\ell$ beads and antibody was tapped for mix, and spun down. After the incubation on ice for 30 min, the tube was spun down, and set to the magnet holder. After the beads were attracted by the magnet, the supernatant was discarded and the tube was removed for the holder. 22 $\mu\ell$ 5mg/ml BSA in PBS was added to the tube and mixed. The tube was set to the magnet holder. After the beads were attracted by the magnet, the supernatant was discarded. This beads wash step was repeated total three times. After final supernatant was discarded, 33 $\mu\ell$ 5mg/ml BSA in FA Lysis buffer was added to the tube, tapped for mix, and spun down. The tube was rotated for 1h at 4^o C. After the tube was spun down, the

tube was set to the magnet holder. After the beads were attracted by the magnet, the supernatant was discarded and 110 $\mu\ell$ ice-cold FA Lysis buffer was added, tapped for mix, and spun down. After the tube was spun down, the tube was set to the magnet holder. After the beads were attracted by the magnet, the supernatant was discarded and 11 $\mu\ell$ ice-cold FA Lysis buffer was added, tapped for mix, spun down and put on ice. 240 $\mu\ell$ WCE was added to the new tube, and the 11 $\mu\ell$ beads-antibody solution was suspended. The tube was rotated for 90 min at 4 °C. After the rotation, the tube was spun down. Then, the tube was set to the magnet holder. After the beads were attracted by the magnet, the supernatant was discarded.

vii) Wash beads

300 $\mu\ell$ ice-cold FA Lysis buffer was added to the tube, tapped for mix, and incubated for 3 min at room temperature. After the incubation, the tube was set to the magnet holder. After the beads were attracted by the magnet, the supernatant was discarded. The wash by ice-cold FA Lysis buffer was repeated again. Next, 300 $\mu\ell$ FA Lysis buffer / NaCl (see Table 5) was added to the tube, tapped for mix, and incubated for 3min at room temperature. After the incubation, the tube was set to magnet holder. After the beads were attracted by the magnet, the supernatant was discarded. The wash by FA Lysis buffer / NaCl was repeated again. Then, 300 $\mu\ell$ ChIP wash buffer (see Table 5) was added to the tube, tapped for mix, and incubated for 3 min at room temperature. After the incubation, the tube was set to the magnet holder. After the beads were attracted by the magnet, the supernatant was discarded. The wash by ChIP wash buffer was

repeated again. Finally, 300 $\mu\ell$ TE buffer (pH 7.5) was added to the tube, tapped for mix, and incubated for 3 min at room temperature. After the incubation, the tube was set to magnet holder. After the beads were attracted by the magnet, the supernatant was discarded. The wash by TE buffer was repeated again.

viii) Elute protein from beads

50 $\mu\ell$ ChIP elution buffer was added to the tube, tapped for dissolution, and spun down. After mild tapping, the tube was incubated for 10 min at 65 °C. Then the tube was tapped mildly, and spun down. The tube was set to the magnet holder. After the beads were attracted by the magnet, the supernatant was used for reverse cross-link to purify DNA.

ix) Reverse cross-link and purify DNA

40 $\mu\ell$ TE buffer (pH 7.5) and 10 $\mu\ell$ 20 mg/ml proteinase K in TBS were added to the supernatant in a new tube. Total 100 $\mu\ell$ solution was incubated for 2 h at 37 °C and for 6 h at 65 °C. This sample was treated as immunoprecipitated (IP) sample. In addition, 50 $\mu\ell$ ChIP elution buffer, 40 $\mu\ell$ TE buffer (pH 7.5) and 10 $\mu\ell$ 20 mg/ml proteinase K in TBS were added to the whole cell extract (input). This solution was also incubated for 2 h at 37 °C and for 6 h at 65 °C. After the incubation, 8 $\mu\ell$ 5M LiCl was added to the tube. DNA was extracted by phenol chloroform and precipitated by ethanol. After 70% ethanol wash, dried pellet was suspended into 30 $\mu\ell$ TE buffer (pH 8.0).

x) Quantitative PCR and agarose gel electrophoresis

The input and IP samples were analyzed by quantitative PCR (qPCR). To confirm that PCR reaction is in the linear range, input and IP samples were serially two-fold diluted and the PCR products were separated on 2.0 % agarose gels and stained with ethidium bromide. The values are given as a percentage of immunoprecipitates (IP/input). Four regions in the rDNA were analyzed by qPCR. Primer sequences were described previously (Ide *et al.*, 2010) and shown in Table 4.

7. References

- Adkins NL, Niu H, Sung P, Peterson CL. (2013):** Nucleosome dynamics regulates DNA processing. *Nat Struct Mol Biol.* 20:836-842
- Antoniacci LM, Kenna MA, Skibbens RV. (2007):** The nuclear envelope and spindle pole body-associated Mps3 protein bind telomere regulators and function in telomere clustering. *Cell Cycle.* 6:75-79
- Aparicio O, Geisberg J, Struhl K. (2005):** Chromatin immunoprecipitation for determining the association of proteins with specific genomic sequences in vivo. *Current Protocols in Cell Biology* 17.7.1-17.7.23
- Bairwa NK, Mohanty BK, Stamenova R, Curcio MJ, Bastia D. (2011):** The intra-S phase checkpoint protein Tof1 collaborates with the helicase Rrm3 and F-box protein Dia2 to maintain genome stability in *Saccharomyces cerevisiae*. *J Biol Chem.* 286:2445-2454
- Branzei D and Foiani M. (2010):** Maintaining genome stability at the replication fork. *Nat Rev Mol Cell Biol.* 11:208-219
- Bupp JM, Martin AE, Stensrud ES, Jaspersen SL. (2007):** Telomere anchoring at the nuclear periphery requires the budding yeast Sad1-UNC-84 domain protein Mps3. *J Cell Biol.* 179:845-854
- Burgess RC, Rahman S, Lisby M, Rothstein R, Zhao X. (2007):** The Slx5-Slx8 complex affects sumoylation of DNA repair proteins and negatively regulates recombination. *Mol Cell Biol.* 27:6153-6162
- Burkhalter MD and Sogo JM. (2004):** rDNA enhancer affects replication initiation and mitotic recombination: Fob1 mediates nucleolytic processing independently of replication. *Mol Cell.* 15:409-421
- Cook CE, Hochstrasser M, Kerscher O. (2009):** The SUMO-targeted ubiquitin ligase subunit Slx5 resides in nuclear foci and at sites of DNA breaks. *Cell Cycle.* 8:1080-1089
- Cuperus G, Shafaatian R, Shore D. (2000):** Locus specificity determinants in the multifunctional yeast silencing protein Sir2. *EMBO J.* 19:2641-2651

Dan Burke D D and Tim Stearns (2000): Methods in Yeast genetics, ED. 2000. *COLD SPRING HARBOR LABORATORY PRESS*.

Doksani Y, Bermejo R, Fiorani S, Haber J E, Foiani M. (2009): Replication dynamics, dormant origin firing, and terminal fork integrity after double-strand break formation. *Cell*. 137:247-258

Doksani Y, Bermejo R, Fiorani S, Haber JE, Foiani M. (2009): Replicon dynamics, dormant origin firing, and terminal fork integrity after double-strand break formation. *Cell*. 137:247-258

Eckert-Boulet N and Lisby M. (2009): Regulation of rDNA stability by sumoylation. *DNA repair*. 8:507-516

Economopoulou P, Dimitriadis G, Psyrris A. (2015): Beyond BRCA: new hereditary breast cancer susceptibility genes. *Cancer Treat Rev*. 41:1-8

Friedel AM, Pike BL, Gasser SM. (2009): ATR/Mec1: coordinating fork stability and repair. *Curr Opin Cell Biol*. 21:237-244

Ganley AR, Ide S, Saka K, Kobayashi T. (2009): The effect of replication initiation on gene amplification in the rDNA and its relationship to aging. *Mol Cell*. 35:683-693

Ganley ARD, Ide S, Saka K, Kobayashi T. (2009): The effect of replication initiation on gene amplification in the rDNA and its relationship to aging. *Mol Cell*. 35:683-693

Gotta M, Laroche T, Formenton A, Maillet L, Scherthan H, Gasser SM. (1996): The clustering of telomeres and colocalization with Rap1, Sir3, and Sir4 proteins in wild-type *Saccharomyces cerevisiae*. *J. Cell Biol*. 143:1349-1363

Horigome C, Oma Y, Konishi T, Schmid R, Marcomini I, Hauer MH, Dion V, Harata M, Gasser SM. (2014): SWR1 and INO80 chromatin remodelers contribute to DNA double-strand break perinuclear anchorage site choice. *Mol Cell*. 55:626-639

Huang J, Brito IL, Villen J, Gygi SP, Amon A, Moazed D. (2006): Inhibition of homologous recombination by a cohesion-associated clamp complex recruited to the rDNA recombination enhancer. *Genes Dev*. 20:2887-2901

Ide S and Kobayashi T. (2010): Analysis of DNA replication in *Saccharomyces cerevisiae* by two-dimensional and pulsed-field gel electrophoresis. *Current Protocols in Cell Biology*

Ide S, Miyazaki T, Maki H, Kobayashi T. (2010): Abundance of ribosomal RNA gene copies maintains genome integrity. *Science* 327:693-696

Ivessa AS, Zhou JQ, Zakian VA. (2000): The *Saccharomyces* Pif1p DNA helicase and the highly related Rrm3p have opposite effects on replication fork progression in ribosomal DNA. *Cell*. 100:479-489

Jackson JD and Gorovsky MA. (2000): Histone H2A.Z has a conserved function that is distinct from that of the major H2A sequence variants. *Nucleic Acids Res.* 28:3811-3816

Jaspersen SL and Ghosh S. (2012): Nuclear envelope insertion of spindle pole bodies and nuclear pore complexes. *Nucleus*. 3:226-236

Jaspersen SL, Giddings TH Jr, Winey M. (2002): Mps3p is a novel component of the yeast spindle pole body that interacts with the yeast centrin homologue Cdc13p. *J Cell Biol.* 159:945-956

Johzuka K and Horiuchi T. (2009): The cis element and factors required for condensin recruitment to chromosomes. *Mol Cell.* 34:26-35

Kobayashi T, Heck DJ, Nomura M, Horiuchi T. (1998): Expansion and contraction of ribosomal DNA repeats in *Saccharomyces cerevisiae*: requirement of replication fork blocking (Fob1) protein and the role of RNA polymerase I. *Genes Dev.* 12:3821-3830

Kobayashi T, Nomura M, Horiuchi T. (2001): Identification of DNA cis elements essential for expansion of ribosomal DNA repeats in *Saccharomyces cerevisiae*. *Mol Cell Biol.* 21:136-147

Kobayashi T, Horiuchi T, Tongaonkar P, Vu L, Nomura M. (2004): SIR2 regulates recombination between different rDNA repeats, but not recombination within individual rRNA genes in yeast. *Cell* 117:441-453

Kobayashi T. (2006): Strategies to maintain the stability of the ribosomal RNA gene repeats –Collaboration of recombination, cohesion, and condensation- *Genes Genet. Syst.* 81:155-161.

Kruhlak M, Crouch EE, Orlov M, Montañó C, Gorski SA, Nussenzweig A, Misteli T, Phair RD, Casellas R. (2007): The ATM repair pathway inhibits RNA polymerase I transcription in response to chromosome breaks. *Nature.* 447:730-734

Lee CS, Lee K, Legube G, Haber JE. (2014): Dynamics of yeast histone H2A and H2B phosphorylation in response to a double-strand break. *Nat Struct Mol Biol.* 21:103-109

Lewinska A, Miedziak B, Kulak K, Molon M, Wnuk M. (2014): Links between nucleolar activity, rDNA stability, aneuploidy and chronological aging in the yeast *Saccharomyces cerevisiae*. *Biogerontology.* 15:289-316

Longhese M P, Bonetti D, Manfrini N, Clerici M. (2010): Mechanisms and regulation of DNA end resection. *EMBO J.* 29:2864-2874

Lopes M, Cotta-Ramusino C, Pellicoli A, Liberi G, Plevani P, Muzi-Falconi M, Newlon CS, Foiani M. (2001): The DNA replication checkpoint response stabilizes stalled replication forks. *Nature.* 412:557-561

Luk E, Ranjan A, Fitzgerland PC Mizuguchi G, Huang Y, Wei D, Wu C. (2010): Stepwise histone replacement by SWR1 requires dual activation with histone H2A.Z and canonical nucleosome. *Cell.* 143:725-736

Mekhail K and Moazed D. (2010): The nuclear envelop in genome organization, expression and stability. *Nat Rev Mol Cell Biol.* 11:317-328

Mekhail K, Seebacher J, Gygi SP, Moazed D. (2008): Role for perinuclear chromosome tethering in maintenance of genome stability. *Nature* 456:667-670

Mimitou EP and Symington LS. (2010): Ku prevents Exo1 and Sgs1-dependent resection of DNA ends in the absence of a functional MRX complex or Sae2. *EMBO J* 29:3358-3369

Miyazaki T and Kobayashi T. (2011): Visualization of the dynamic behavior of ribosomal RNA gene repeats in living yeast cells. *Genes to Cells* 16:491-502

Mizuguchi G, Shen X, Landry J, Wu WH, Sen S, Wu C. (2004): ATP-driven exchange of histone H2AZ variant catalyzed by SWR1 chromatin remodeling complex. *Science.* 303:343-348

Morrison AJ and Shen X. (2009): Chromatin remodeling beyond transcription: the INO80 and SWR1 complexes. *Nat Rev Mol Cell Biol.* 10:373-384

Mundbjerg K, Jørgensen SW, Fredsøe J, Nielsen I, Pedersen JM, Bentsen IB, Lisby M, Bjerbaek L, Andersen AH. (2015): Top2 and Sgs1-Top3 Act Redundantly to Ensure rDNA

Replication Termination. *PLoS Genet.* 11:e1005697

Nagai S, Davoodi N, Gasser SM. (2011): Nuclear organization in genome stability: SUMO connections. *Cell Res.* 21:474-485

Nagai S, Dubrana K, Tsai-Pflugfelder M, Davidson M B, Roberts T M, Brown G W, Varela E, Hediger F, Gasser S M, Krogan N J. (2008): Functional targeting of DNA damage to a nuclear pore-associated SUMO-dependent ubiquitin ligase. *SCIENCE* 322:597-602

Nishikawa S, Terazawa Y, Nakayama T, Hirata A, Makio T, Endo T. (2003): Nep98p is a component of the yeast spindle pole body and essential for nuclear division and fusion. *J Cell Biol.* 278:9938-9943

Osakabe A, Takahashi Y, Murakami H, Otawa K, Tachiwana H, Oma Y, Nishijima H, Shibahara KI, Kurumizaka H, Harata M. (2014): DNA binding properties of the actin-related protein Arp8 and its role in DNA repair. *PLoS One.* 9:e108354

Oza P, Jaspersen SL, Miele A, Dekker J, Peterson CL. (2009): Mechanisms that regulate localization of a DNA double-strand break to the nuclear periphery. *Genes Dev.* 23:912-927

Palladino F, Laroche T, Gilson E, Axelrod A, Pillus L, Gasser SM. (1993): SIR3 and SIR4 proteins are required for the positioning and integrity of yeast telomeres. *Cell.* 75:543-555

Papamichos-Chronakis M, Krebs JE, Peterson CL. (2006): Interplay between Ino80 and Swr1 chromatin remodeling enzymes regulates cell cycle checkpoint adaptation in response to DNA damage. *Genes Dev.* 20:2437-2449

Pelliccioli A and Foiani M. (2005): Signal transduction: how rad53 kinase is activated. *Curr Biol.* 15:769-771

Sabourin M and Zakian V A. (2008): ATM-like kinases and regulation of telomerase: lessons from yeast and mammals. *Trends in Cell Biology* 18:337-346

Sambrook J and Russell D W. (2001): Molecular Cloning A LABORATORY MANUAL THIRD EDITION. *COLD SPRING HARBOR LABORATORY PRESS.*

Seeber A, Hauer M, Gasser SM. (2013): Nucleosome remodelers in double-strand break repair. *Curr Opin Genet Dev.* 23:174-184

Sheedy DM, Dimitrova D, Rankin JK, Bass KL, Lee KM, Tapia-Alveal C, Harvey SH, Murray JM, O'Connell MJ. (2005): Brcl-mediated DNA repair and damage tolerance. *Genetics*. 171:457-468

Shimada K, Oma Y, Schleker T, Kugou K, Ohta K, Harata M, Gasser SM. (2008): Ino80 chromatin remodeling complex promotes recovery of stalled replication forks. *Curr Biol*. 18:566-575

Shore D and Bianchi A. (2009): Telomere length regulation: coupling DNA end processing to feedback regulation of telomerase. *EMBO J*. 28:2309-2322

Shroff R, Arbel-Eden A, Plich D, Ira G, Bonner WM, Petrini JH, Haber JE, Lichten M. (2004): Distribution and dynamics of chromatin modification induced by a defined DNA double-strand break. *Curr Biol*. 14:1703-1711

Strambio-De-Castillia C, Niepel M, Rout MP. (2010): The nuclear pore complex: bridging nuclear transport and gene regulation. *Nat Rev Mol Cell Biol*. 11:490-501

Taddei A, Schober H, Gasser SM. (2010): The budding yeast nucleus. *Cold Spring Harb Perspect Biol*. 2:a000612

Torres-Rosell J, Sunjevaric I, De Piccoli G, Sacher M, Eckert-Boulet N, Reid R, Jentsch S, Rothstein R, Aragon L, Lisby M. (2007): The Smc5-Smc6 complex and SUMO modification of Rad52 regulates recombinational repair at the ribosomal gene locus. *Nat Cell Biol*. 9:923-931

Tourriere H and Pasero P. (2007): Maintenance of fork integrity at damaged DNA and natural pause sites. *DNA repair*. 6:900-913

Turinetto V and Giachino C. (2015): Multiple facets of histone variant H2AX: a DNA double-strand-break marker with several biological functions. *Nucleic Acids Res*. 43:2489-2498

van Attikum H, Fritsch O, Gasser SM (2007): Distinct roles for SWR1 and INO80 chromatin remodeling complexes at chromosomal double-strand breaks. *EMBO J*. 26:4113-4125

van Attikum H, Fritsch O, Hohn B, Gasser SM. (2004): Recruitment of the INO80 complex by H2A phosphorylation links ATP-dependent chromatin remodeling with DNA double-strand break repair. *Cell*. 119:777-788

Voineagu I, Narayanan V, Lobachev KS, Mirkin SM. (2008): Replication stalling at unstable

inverted repeats: interplay between DNA hairpins and fork stabilizing proteins. *Proc Natl Acad Sci USA*. 105:9936-9941

Yao W, Beckwith SL, Zheng T, Young T, Dinh VT, Ranjan A, Morrison AJ. (2015): Assembly of the Arp5 (Actin-related Protein) Subunit Involved in Distinct INO80 Chromatin Remodeling Activities. *J Biol Chem*. 290:25700-25709

Zhang C, Roberts TM, Yang J, Desai R, Brown GW. (2006): Suppression of genomic instability by SLX5 and SLX8 in *Saccharomyces cerevisiae*. *DNA repair*. 5:336-346

Zhao X, Georgieva B, Chabes A, Domkin V, Ippel JH, Schleucher J, Wijmenga S, Thelander L, Rothstein R. (2000): Mutational and structural analyses of the ribonucleotide reductase inhibitor Sml1 define its Rnr1 interaction domain whose inactivation allows suppression of *mec1* and *rad53* lethality. *Mol Cell Biol*. 20:9076-9083

Table 1. Yeast strains used in this study

Name	Background	Genotype	Source
WT	W303	<i>MAT a leu2-3, 112 trp1-1 can1-100 ura3-1 ade2-1 his3-11.15</i>	NOY408-1b
<i>fob1</i>	W303	<i>MAT a leu2-3, 112 trp1-1 can1-100 ura3-1 ade2-1 his3-11.15 fob1::LEU2</i>	This study
<i>tell</i>	W303	<i>MAT a leu2-3, 112 trp1-1 can1-100 ura3-1 ade2-1 his3-11.15 tellΔ::kanMX6</i>	This study
<i>fob1 tell</i>	W303	<i>MAT a leu2-3, 112 trp1-1 can1-100 ura3-1 ade2-1 his3-11.15 tellΔ::kanMX6</i>	This study
<i>sir2</i>	W303	<i>MAT a leu2-3, 112 trp1-1 can1-100 ura3-1 ade2-1 his3-11.15 sir2Δ::kanMX6</i>	This study
<i>nup84</i>	W303	<i>MAT a leu2-3, 112 trp1-1 can1-100 ura3-1 ade2-1 his3-11.15 nup84::LEU2</i>	This study
<i>arp5</i>	W303	<i>MAT a leu2-3, 112 trp1-1 can1-100 ura3-1 ade2-1 his3-11.15 arp5Δ::kanMX6</i>	This study
<i>tof2</i>	W303	<i>MAT a leu2-3, 112 trp1-1 can1-100 ura3-1 ade2-1 his3-11.15 tof2Δ::kanMX6</i>	This study
<i>csm1</i>	W303	<i>MAT a leu2-3, 112 trp1-1 can1-100 ura3-1 ade2-1 his3-11.15 csm1Δ::kanMX6</i>	This study
<i>lrs4</i>	W303	<i>MAT a leu2-3, 112 trp1-1 can1-100 ura3-1 ade2-1 his3-11.15 lrs4Δ::kanMX6</i>	This study
<i>tof1</i>	W303	<i>MAT a leu2-3, 112 trp1-1 can1-100 ura3-1 ade2-1 his3-11.15 tof1Δ::kanMX6</i>	This study
<i>rrm3</i>	W303	<i>MAT a leu2-3, 112 trp1-1 can1-100 ura3-1 ade2-1 his3-11.15 rrm3Δ::kanMX6</i>	This study
<i>hta1 S129A, hta2 S129A</i>	W303	<i>MAT a leu2-3, 112 trp1-1 ura3-1 ade2-1 his3-11.15 hta1 S129A hta2 S129A</i>	from Dr. Shimada
<i>sml1 mec1</i>	W303	<i>MAT a leu2-3, 112 trp1-1 ura3-1 ade2-1 his3-11.15 sml1::HIS3 mec1::ADE2</i>	from Dr. Kanemaki
<i>sml1 mec1 tell</i>	W303	<i>MAT a leu2-3, 112 trp1-1 ura3-1 ade2-1 his3-11.15 sml1::HIS3 mec1::ADE2</i>	This study
<i>mps3 Δ N</i>	W303	<i>MAT a leu2-3, 112 trp1-1 can1-100 ura3-1 ade2-1 his3-11.15 mps3 Δ 65-145</i>	Horigome <i>et al.</i> , 2014
<i>htz1</i>	W303	<i>MAT a leu2-3, 112 trp1-1 can1-100 ura3-1 ade2-1 his3-11.15 htz1Δ::kanMX6</i>	This study
<i>slx5</i>	W303	<i>MAT a leu2-3, 112 trp1-1 can1-100 ura3-1 ade2-1 his3-11.15 slx5Δ::kanMX6</i>	This study
<i>slx8</i>	W303	<i>MAT a leu2-3, 112 trp1-1 can1-100 ura3-1 ade2-1 his3-11.15 slx8Δ::kanMX6</i>	This study
WT Nup84-FLAG	W303	<i>MAT a leu2-3, 112 trp1-1 can1-100 ura3-1 ade2-1 his3-11.15 10FLAG-NUP84</i>	This study
<i>fob1</i> Nup84-FLAG	W303	<i>MAT a leu2-3, 112 trp1-1 can1-100 ura3-1 ade2-1 his3-11.15 fob1::LEU2 10FLAG-</i>	This study
WT Mps3-FLAG	W303	<i>MAT a leu2-3, 112 trp1-1 can1-100 ura3-1 ade2-1 his3-11.15 10FLAG-MPS3</i>	This study
<i>fob1</i> Mps3-FLAG	W303	<i>MAT a leu2-3, 112 trp1-1 can1-100 ura3-1 ade2-1 his3-11.15 fob1::LEU2 10FLAG-</i>	This study
WT Ycplac33	W303	<i>MAT a leu2-3, 112 trp1-1 can1-100 ura3-1 ade2-1 his3-11.15 Ycplac33</i>	This study
<i>fob1::LEU2</i> Ycplac33	W303	<i>MAT a leu2-3, 112 trp1-1 can1-100 ura3-1 ade2-1 his3-11.15 fob1::LEU2 Ycplac33</i>	This study
<i>fob1::LEU2</i> Ycplac33- <i>FOB1</i>	W303	<i>MAT a leu2-3, 112 trp1-1 can1-100 ura3-1 ade2-1 his3-11,15 fob1::LEU2 Ycplac33-</i>	This study

Table 2. Plasmids used in this study

Name	Description	Marker	Reference
pUC19			
pUC19- <i>fob1::LEU2</i>			
pRS305		<i>LEU2</i>	
Ycplac33		<i>URA3</i>	
Ycplac33- <i>FOB1</i>		<i>URA3</i>	This study
pRS306- <i>mps3</i> Δ 65-145	Plasmid containing <i>MPS3</i> promoter, <i>mps3</i> Δ 65-145 and <i>MPS3</i> terminator	<i>URA3</i>	Horigome <i>et al.</i> , 2011

Table 3. Media used for yeast cell culture

Name	Constituents	Final concentration
YPD ^{1 2}	Bacto yeast extract	10 g/L
	Bacto Peptone	20
	D-glucose	20
	Bacto agar ³	20
SC ^{1 2 4}	Bacto-yeast nitrogen base (without amino acids)	6.7
	Drop out mix ⁵	0.2
	Supplements ⁶	
	D-glucose	20
	Bacto agar ³	20

1; For YP-Galactose and S-Galactose medium, 2% D-glucose was replaced with 2% D-galactose

2; To culture or select drug resistance strains, G418 was added with the concentration shown below

G418	500ug/ml	Sigma
------	----------	-------

3; For plate medium

4; For the selection of ura3- cells, 5-Fluoroorotic Acid (5-FOA) was added with the concentration shown below

5-FOA	0.1% (w/v)	WAKO
-------	------------	------

5; Drop out mix

Constituents	Final concentration
	mg/ml
Adenine sulfate	20
L-Arginine	20
L-Methionine	20
L-Tyrosine	30
L-Isoleucine	30
L-Lysine	30
L-Phenylalanine	50
L-Glutamic acid	100
L-Asparatic acid	100
L-Valine	150
L-Threonine	200
L-Serine	400

6; Depends on the experimental purpose, Uracil(f.c. 20mg/ml), L-Tryptophan(f.c. 20mg/ml), L-Histidine(f.c. 20mg/ml), and L-Leucine(f.c. 100mg/ml) were supplied

Table 4. PCR primers used in this study

Name	Sequence (5'-3')	Size (bp)	Comment
<i>• Primers used for ChIP assay</i>			
ChIP-primer2f	AGGCAGCGTAAAAGGATGAGGCTACT	318	Ide <i>et al.</i> , 2010
ChIP-primer2r	ACTCCGGTTTTGTTCTCTTCCCTCCA		
ChIP-primer4f	ATATGAGGGCAGGGTCCAGACATGTT	256	Ide <i>et al.</i> , 2010
ChIP-primer4r	ACCTGTCACCTTGAAACTACCTCTGC		
ChIP-primer5f	CAGGTTCCACCAAACAGATACC	180	Ide <i>et al.</i> , 2010
ChIP-primer5r	GAAGGATTTGGTGGATTACTAGC		
ChIP-primer8f	TCCCCACCTGACAATGTCTT	134	Ide <i>et al.</i> , 2010
ChIP-primer8r	GCCAGTGAAATACCACTACC		
<i>CUP1</i> -1	TGAAGGTCATGAGTGCCAAT	168	Mekhail <i>et al.</i> , 2008
<i>CUP1</i> -2	TTCGTTTCATTTCCCAGAGCA		
TEL12R-TR1-f	GAGCAACTTGCGTGAATCGAAGACA	210	This study
TEL12R-TR1-r	CGATGATGCCTGCTAAACTGCAGCT		
TEL6R-TR-f	CATTAAAGACACCGCCAAGCTTCCA	270	This study
TEL6R-TR-r	GCGCCTAGTGCAACTAGTGCATATA		
<i>• Primers used for preparing a probe for Chr. XII detection</i>			
rDNAprobe-f1	TCTGAAGAGTTAAGCACTCC		Kobayashi <i>et al.</i> , 2004
rDNAprobe-r1	CTTCCCGAGCGTGAAAGGAT		

Table 5. Buffers used for Southern blotting and hybridization

Name	Constituents		Final Conc.
<i>• Buffers used for Southern blotting</i>			
Denaturation buffer		g/3L	
	NaOH	60	0.5M
	NaCl	262.9	3M
Neutralization buffer		g/3L	
	Tris-HCl (pH = 7.0)	181.7	0.5M
	NaCl	526.5	1.5M
<i>• Buffers used for Southern hybridization</i>			
Hybridization buffer		/40ml	
	BSA	0.4g	50mg/ml
	0.5M EDTA (pH = 8.0)	0.08ml	1mM
	20% SDS	14ml	7%
	1M Na ₂ HPO ₄ (pH = 7.2)	16ml	0.4M
	dH ₂ O	9.92ml	
<i>• ChIP assay</i>			
2.5M Glycine		/100ml	
	Glycine [75.07]	18.77g	2.5M
TBS		/200ml	
	1M Tris-HCl (pH = 7.5)	20ml	0.1M
	NaCl	0.8g	0.40%
PMSF		/1ml	
	PMSF	17.4mg	100mM
5M LiCl		/50ml	
	LiCl	10.6g	5M
FA lysis buffer		/500ml	
	1M HEPES (pH = 7.5)	25ml	50mM
	5M NaCl	15ml	150mM
	0.5M EDTA (pH = 8.0)	1ml	1mM
	100% Triton-X100	5ml	1%
	10% sodium deoxycholate	5ml	0.10%
	20% SDS	2.5ml	0.10%
FA lysis buffer 0.5M NaCl		/100ml	
	1M HEPES (pH = 7.5)	5ml	50mM
	5M NaCl	10ml	0.5M
	0.5M EDTA (pH = 8.0)	0.2ml	1mM
	100% Triton-X100	1ml	1%
	10% sodium deoxycholate	1ml	0.10%
	20% SDS	0.5ml	0.10%
ChIP wash buffer		/200ml	
	1M Tris-HCl (pH = 8.0)	2ml	10mM
	5M LiCl	10ml	0.25M
	0.5M EDTA (pH = 8.0)	0.4ml	1mM
	100% NP-40	1ml	0.50%
	10% sodium deoxycholate	10ml	0.50%
ChIP elution buffer		/200ml	
	1M Tris-HCl (pH = 7.5)	10ml	50mM
	0.5M EDTA (pH = 8.0)	4ml	10mM
	20% SDS	10ml	1%

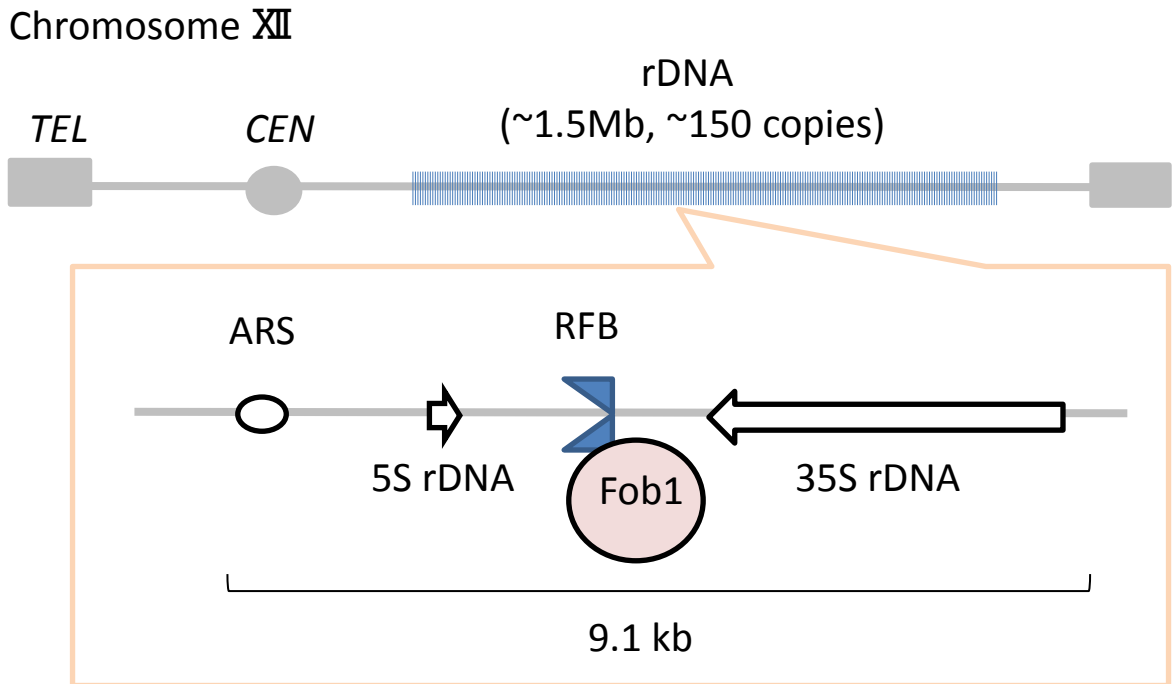


Figure 1. The rDNA encodes genes for structural RNA components of the ribosome in the yeast *Saccharomyces cerevisiae*.

Figure 1. The rDNA encodes genes for structural RNA components of the ribosome in the yeast *Saccharomyces cerevisiae*.

In budding yeast, there are about 150 tandemly repeated copies of the rDNA on Chromosome XII in a haploid cell. The rDNA occupies about 60% of the chromosome. An rDNA repeating unit consists of two rRNA genes (5S and 35S).

The replication fork barrier (RFB) site is in the intergenic spacer between two rRNA genes. Fob1, fork block protein, binds to this site. TEL; telomere, CEN; centromere.

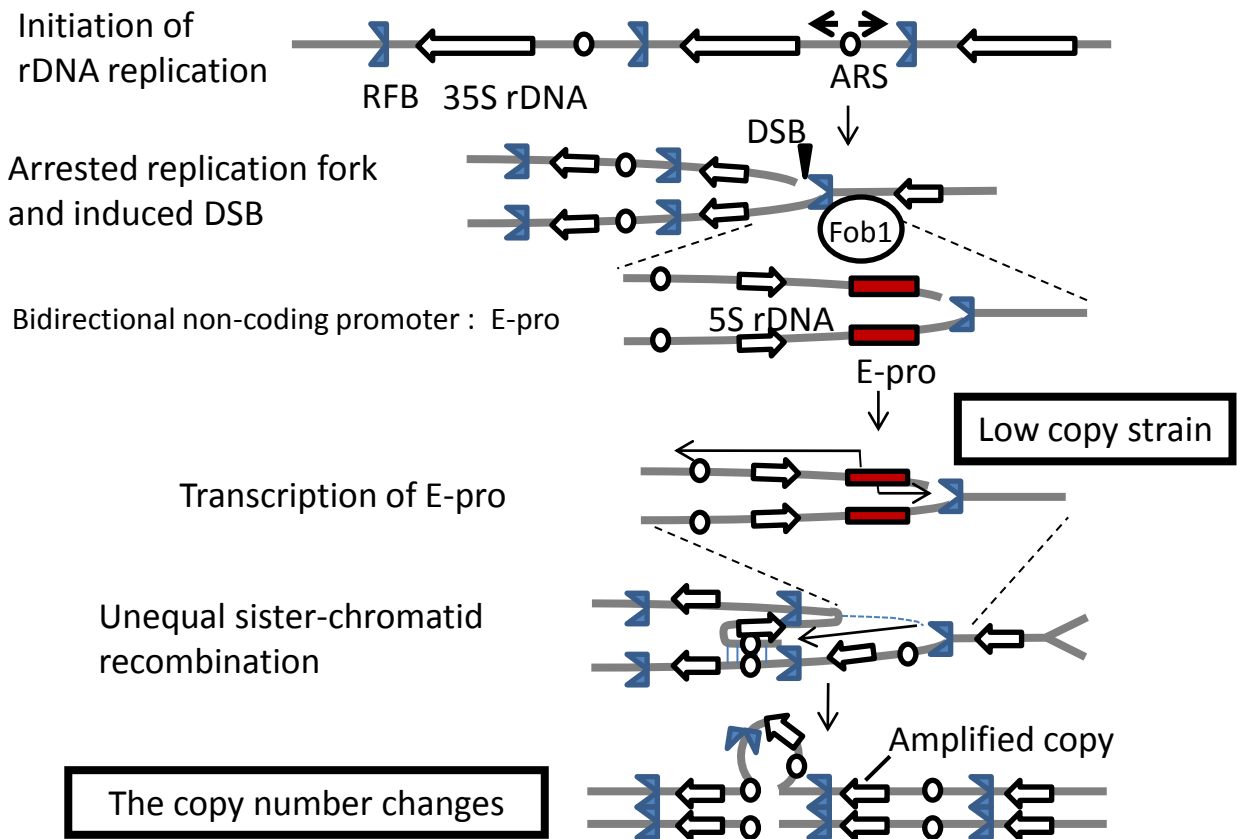


Figure 2. The ribosomal RNA repeated genes (rDNA) in budding yeast has a gene amplification recombination system

Figure 2. The ribosomal RNA repeated genes (rDNA) in budding yeast has a gene amplification recombination system.

The rDNA repeat number is recovered through the DSB repair pathway with sister-chromatid recombination. In this system, at the replication fork barrier (RFB) site which is associated with Fob1, (1)the replication fork is arrested, (2)DNA double-strand break (DSB) is induced, (3)the DSB is repaired by homologous recombination with sister-chromatid, as the results, (4)some copies are replicated twice and (5)the copy number increases.

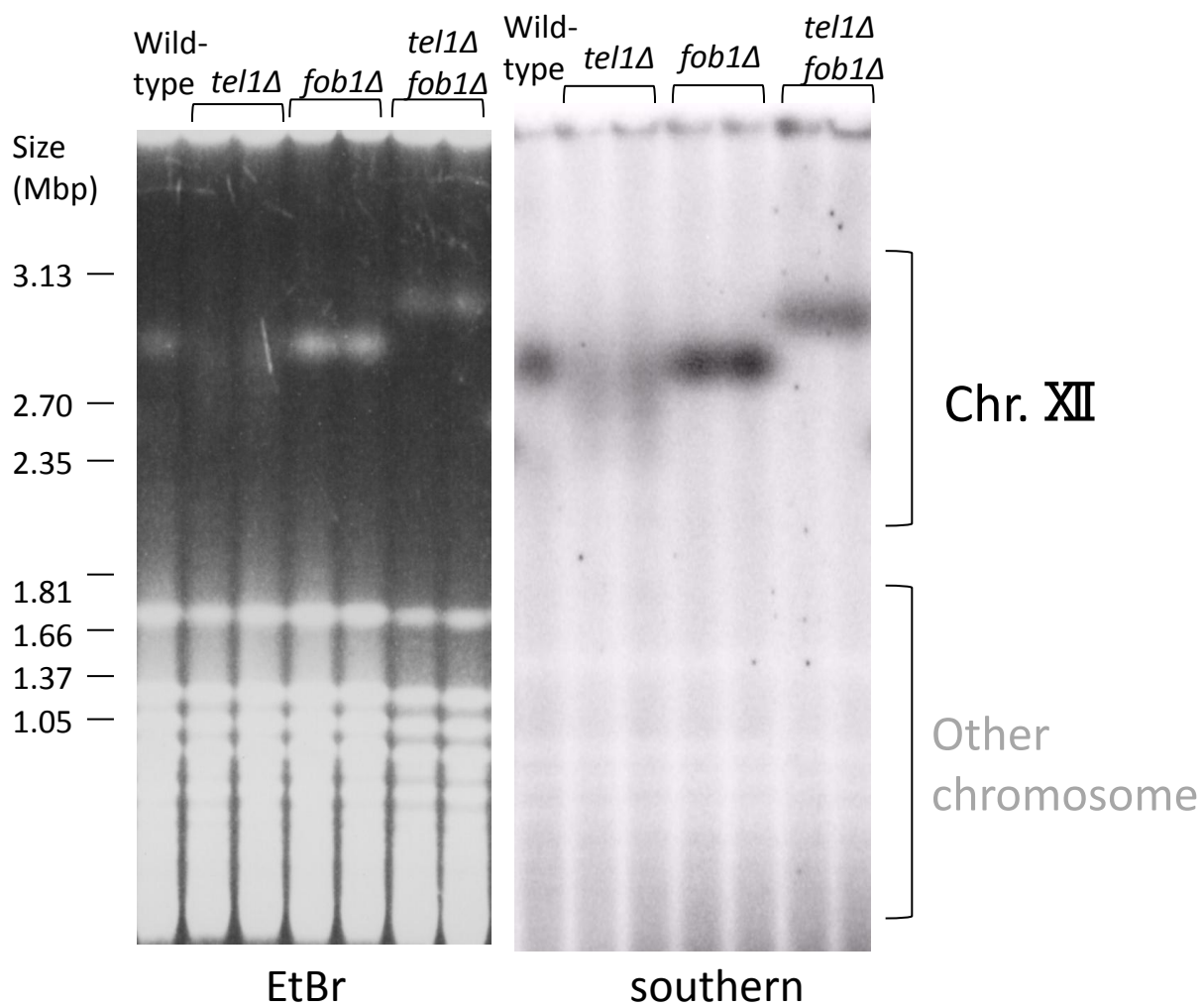


Figure 3. CHEF analysis of rDNA stability in the *tell* mutant.

Figure 3. CHEF analysis of rDNA stability in the *tell* mutant.

Left: ethidium bromide (EtBr) staining of Chr. XII and other chromosomes.

Chromosomes from *S. cerevisiae* cells grown to saturation were resolved on a 0.8% CHEF gel for 68h and gel was stained with ethidium bromide. The size marker is *H. wingei* chromosome. Right: chromosomes resolved by CHEF were analyzed by southern blot using rDNA probe. Chr. XII size in the *tell* mutant was heterogeneous.

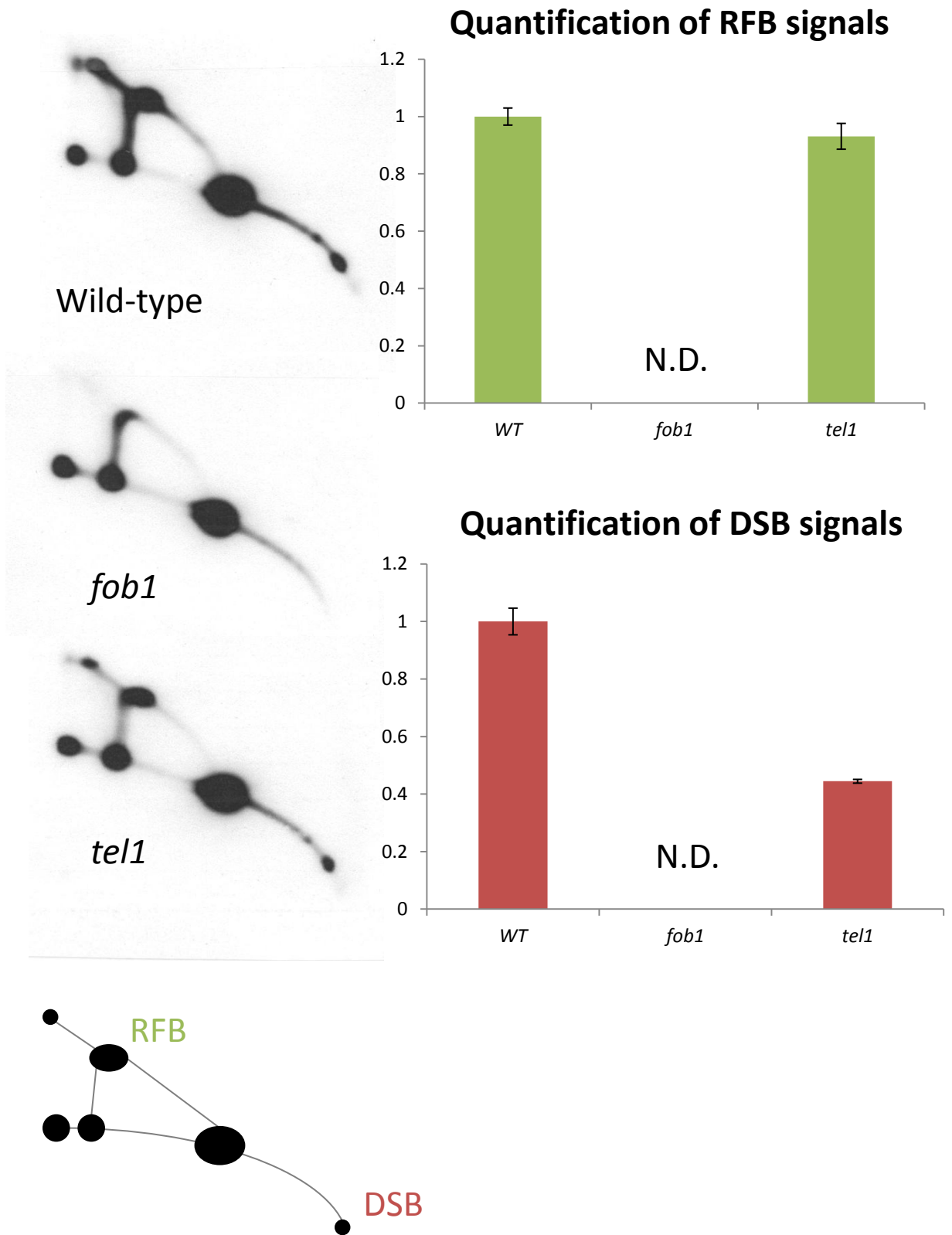


Figure 4. In the *tel1* mutant, the amount of DSBs is less than that of the wild-type.

Figure 4. In the *tell* mutant, the amount of DSBs is less than that of the wild-type. To detect replication and recombination intermediates and DSB spot by 2D gel electrophoresis, DNA was prepared from cells growing in YPD, and digested with Bgl II . The rDNA was detected with an rDNA specific probe. DNA was isolated and digested in plugs. RFB (green) and DSB (red) signals were quantified by ImageQuant (GE). The values obtained for RFB spot were normalized to the values of total replication intermediates signals. The values obtained for DSB spot was normalized to the values of RFB. Average values from three independent experiments are shown in arbitrary units. Wild-type (WT) = 1. N.D. is not-detected in the *fohl* mutant. Error bar shows S.D.(standard deviation).

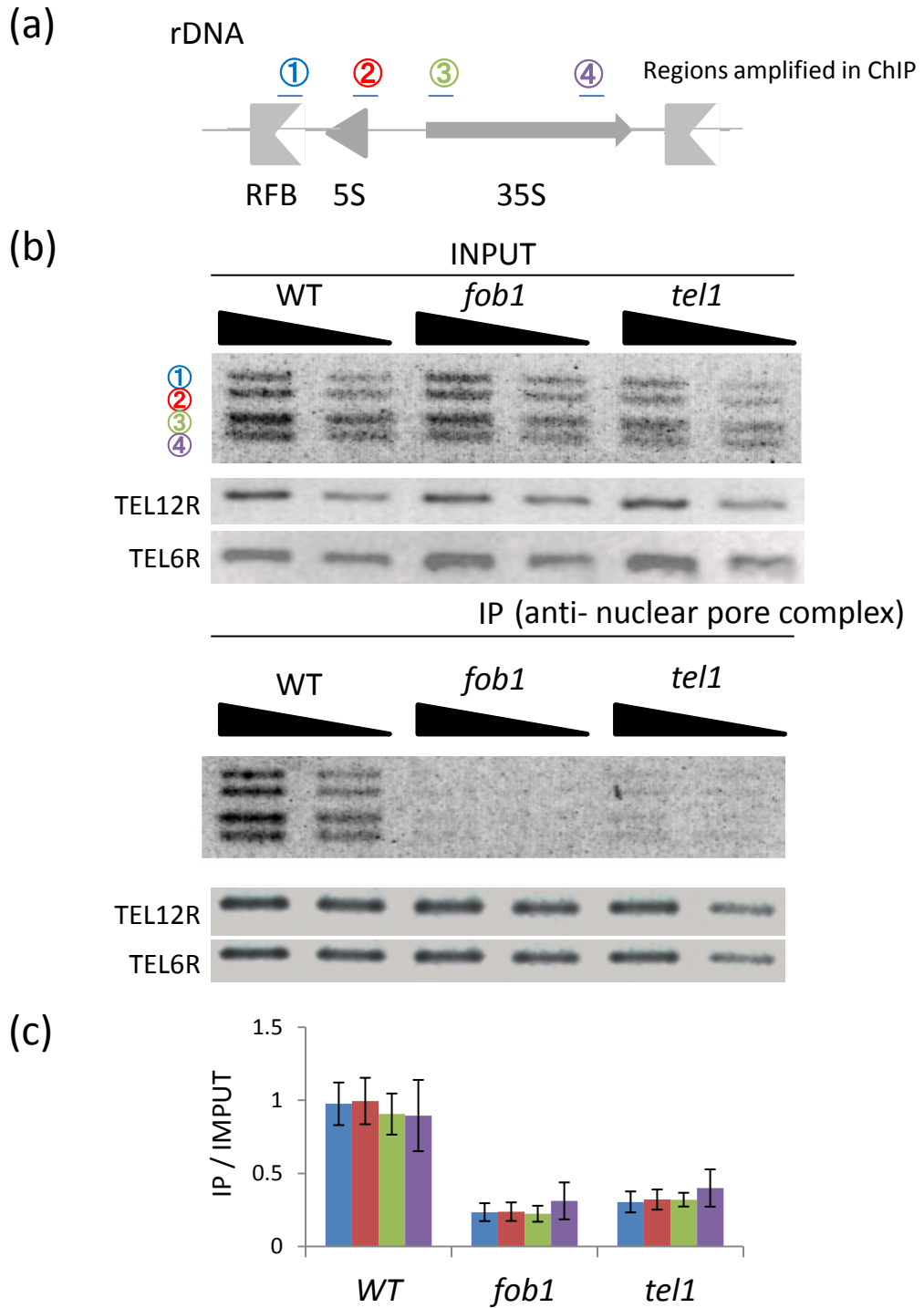
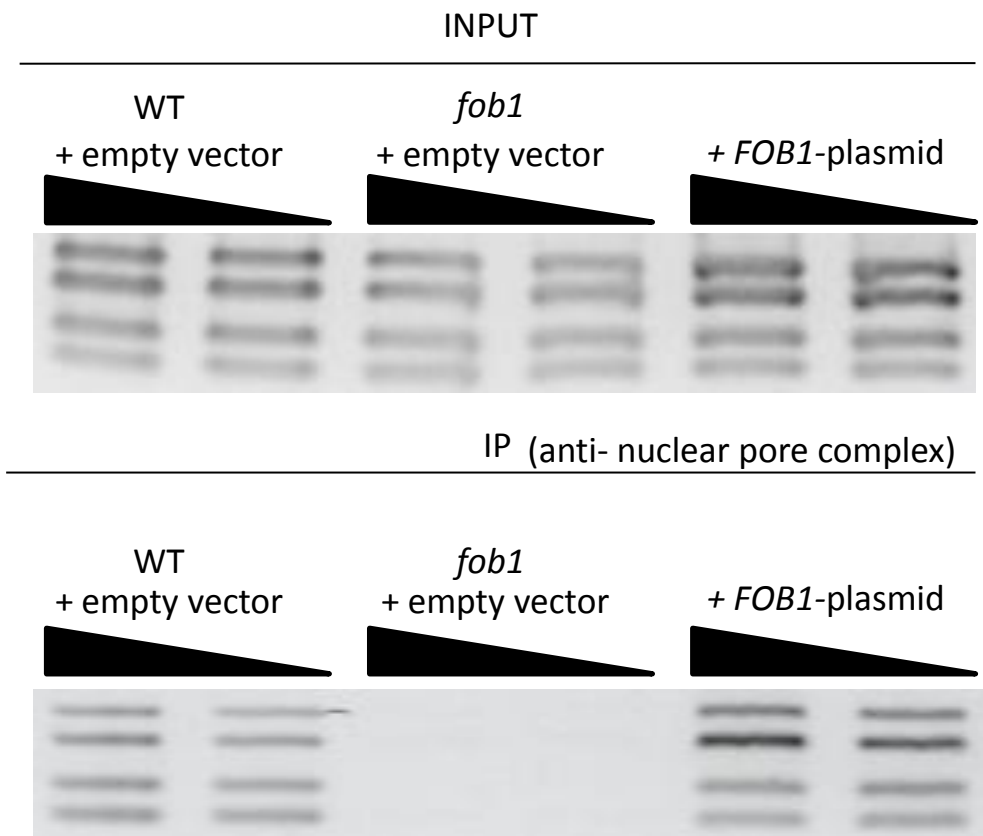


Figure 5. ChIP analysis for rDNA-nuclear pore complex associations in the *fob1* mutant and the *tel1* mutant.

Figure 5. ChIP analysis for rDNA-nuclear pore complex associations in the *fob1* mutant and the *tell* mutant.

(a): Schematic drawing of rDNA and probes used in this assay. RFB, replication fork barrier; 5S, Pol III-transcribed 5S rRNA gene; 35S, Pol I-transcribed 35S rRNA gene. (b): Association of rDNA with the nuclear pore complex(NPC) analyzed by ChIP assays. NOY408-1b (WT, wild-type), the *fob1* mutant(*fob1Δ*) and the *tell* mutant(*tellΔ*) were treated with formaldehyde and DNA associated with NPC was immunoprecipitated with an anti-NPC antibody. Four regions in the rDNA (1 to 4 shown in Figure 2a) as well as control regions, one in telomere of Chr. XII and one in telomere of Chr. VI were analyzed by PCR. PCR products obtained for two sample concentrations (2-fold dilution) were separated on 1.8% agarose gels and stained with ethidium bromide. (c): PCR products shown in (a) and other independent experiments were quantified. The values obtained for immunoprecipitated (IP) DNA were normalized to the values for corresponding input DNAs obtained without IP. Average values from three independent experiments are shown in arbitrary units. Error bars represent standard deviations(means \pm sd).

(a)



(b)

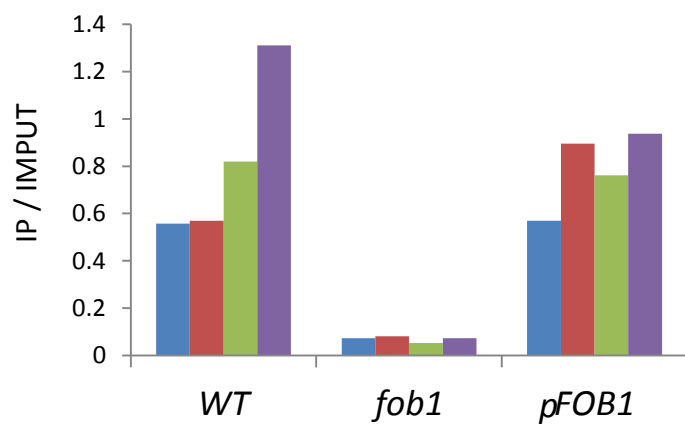


Figure 6. ChIP analysis for rDNA-nuclear pore complex associations in strains which plasmid complementation was carried out

Figure 6. ChIP analysis for rDNA-nuclear pore complex associations and plasmid complementation test

(a): Association of rDNA with the nuclear pore complex(NPC) analyzed by ChIP assays. ChIPs were carried out in NOY408-1b (WT, wild type) with empty vector (pRS306), the *foi1* mutant (*foi1Δ*) with empty vector and the *foi1* mutant (*foi1Δ*) but with intact *FOI1* gene in the plasmid were treated with formaldehyde and DNA associated with NPC was immunoprecipitated with an anti-NPC antibody. Four regions within rDNA (1 to 4 shown in Figure 4a) were analyzed by PCR. PCR products obtained for two sample concentrations (2-fold dilution) were separated on 1.8% agarose gels and stained with ethidium bromide. (b): PCR products shown in (Figure 4a) and other independent experiments were quantified. The values obtained for immunoprecipitated (IP) DNA were normalized to the values for corresponding input DNAs obtained without IP.

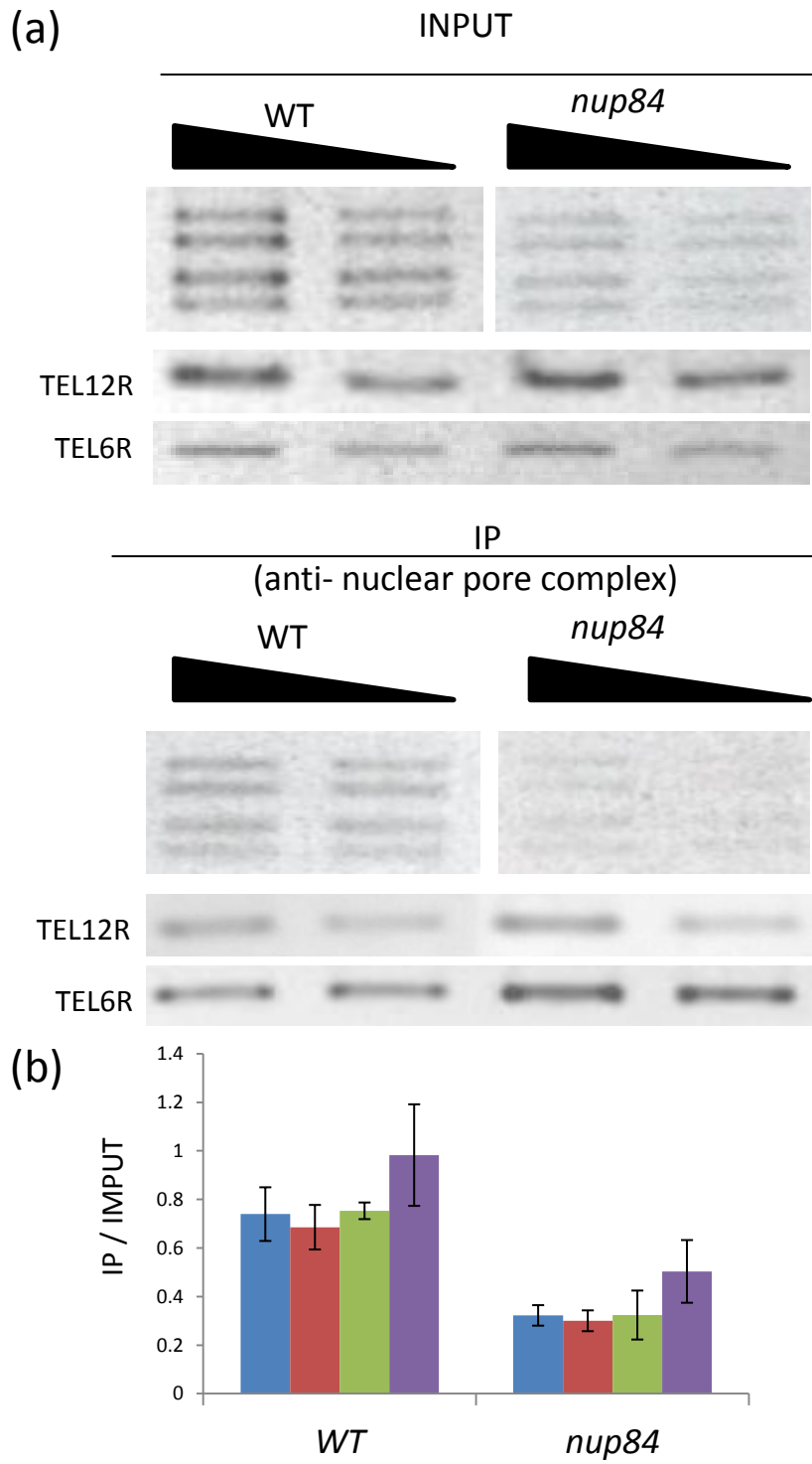
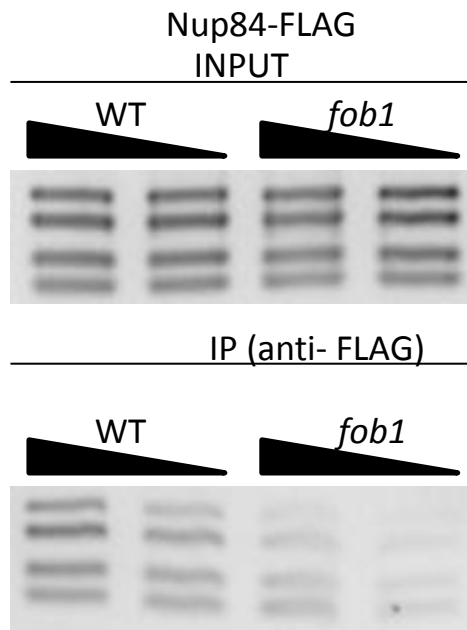


Figure 7. ChIP analysis for rDNA-NPC association in the *nup84* mutant

Figure 7. ChIP analysis for rDNA-NPC association in the *nup84* mutant

(a): Association of rDNA with the nuclear pore complex (NPC) analyzed by ChIP assays. NOY408-1b (WT, wild-type), the *nup84* mutant (*nup84Δ*) were treated with formaldehyde and DNA associated with NPC was immunoprecipitated with an anti-NPC antibody. Four regions within rDNA (1 to 4 shown in Figure 4a) as well as control regions, one at telomere of Chr. XII and one at telomere of Chr. VI were analyzed by PCR. PCR products obtained for two sample concentrations (2-fold dilution) were separated on 1.8% agarose gels and stained with ethidium bromide. (b): PCR products shown in (Figure 4a) and other independent experiments were quantified. The values obtained for immunoprecipitated (IP) DNA were normalized to the values for corresponding input DNAs obtained without IP. Average values from three independent experiments are shown in arbitrary units. Error bars represent standard deviations (means \pm sd).

(a)



(b)

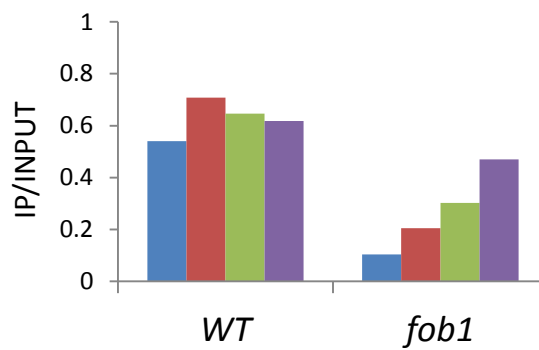


Figure 8. ChIP analysis for rDNA-nuclear pore complex associations in strains which was added FLAG tag in the C-terminus of Nup84

Figure 8. ChIP analysis for rDNA-nuclear pore complex associations in strains which was added FLAG tag in the C-terminus of Nup84

(a): Association of rDNA with Nup84, which is component of NPC, analyzed by ChIP assays. ChIPs were carried out in NOY408-1b (WT, wild type) and the *fab1* mutant (*fab1Δ*) added FLAG tag in the C-terminus of Nup84, respectively. *HIS3* gene was used as marker gene for transformation to add FLAG tag. These cells were treated with formaldehyde and DNA associated with Nup84 was immunoprecipitated with an anti-FLAG antibody. Four regions within rDNA (1 to 4 shown in Figure 4a) were analyzed by PCR. PCR products obtained for two sample concentrations (2-fold dilution) were separated on 1.8% agarose gels and stained with ethidium bromide. (b): PCR products shown in (Figure 4a) and other independent experiments were quantified. The values obtained for immunoprecipitated (IP) DNA were normalized to the values for corresponding input DNAs obtained without IP.

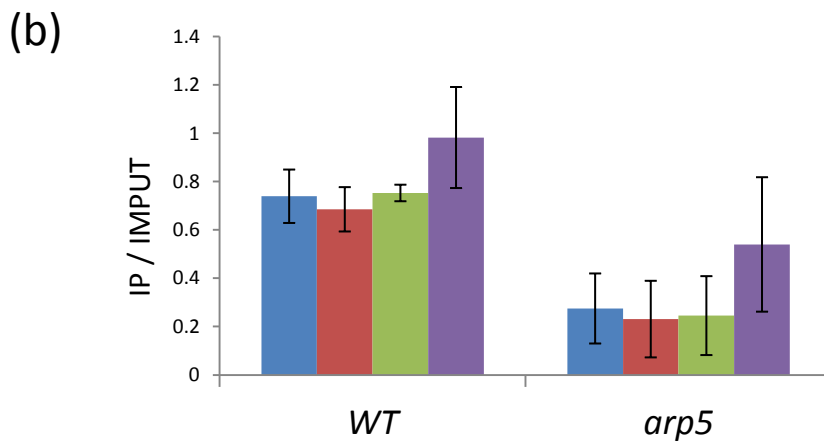
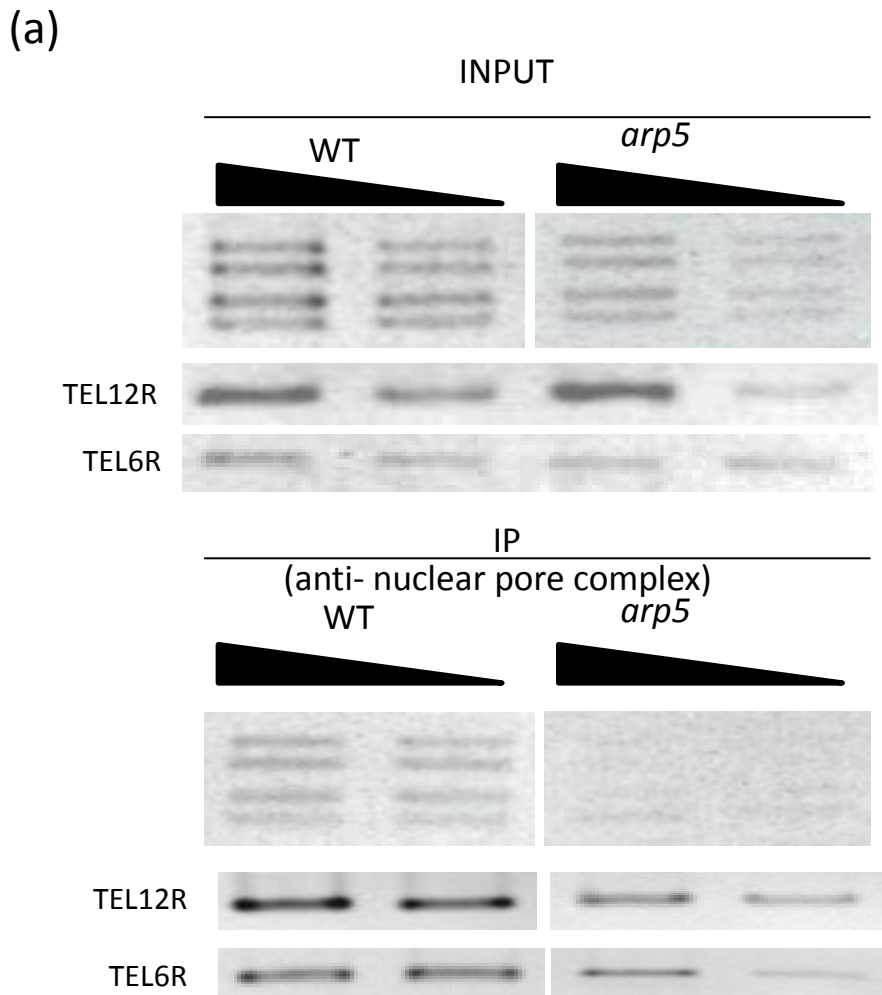


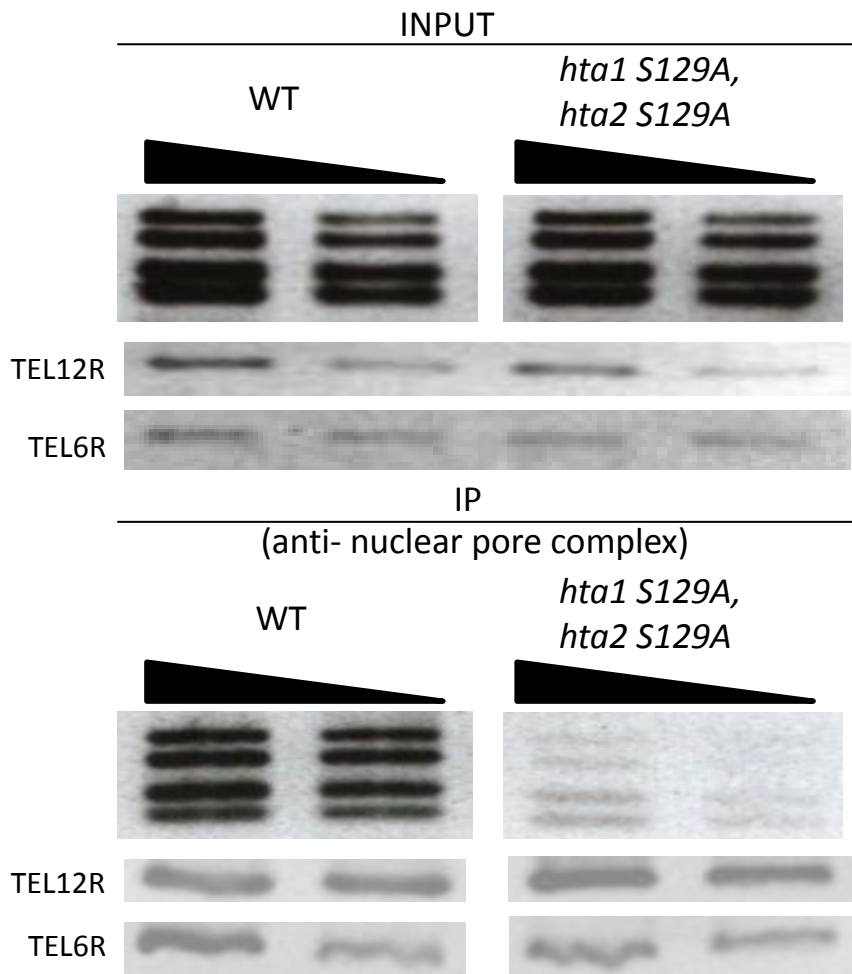
Figure 9. ChIP analysis for rDNA-NPC association in the *arp5* mutant

Figure 9. ChIP analysis for rDNA-NPC association in the *arp5* mutant

(a): Association of rDNA with the nuclear pore complex (NPC) analyzed by ChIP assays. NOY408-1b wild-type, the *arp5* mutant (*arp5Δ*) were treated with formaldehyde and DNA associated with NPC was immunoprecipitated with an anti-NPC antibody. Four regions within rDNA (1 to 4 shown in Figure 4a) as well as control regions, one in telomere of Chr. XII and one in telomere of Chr. VI were analyzed by PCR. PCR products obtained for two sample concentrations (2-fold dilution) were separated on 1.8% agarose gels and stained with ethidium bromide.

(b): PCR products shown in (Figure 4a) and other independent experiments were quantified. The values obtained for immunoprecipitated (IP) DNA were normalized to the values for corresponding input DNAs obtained without IP. Average values from three independent experiments are shown in arbitrary units. Error bars represent standard deviations (means \pm sd).

(a)



(b)

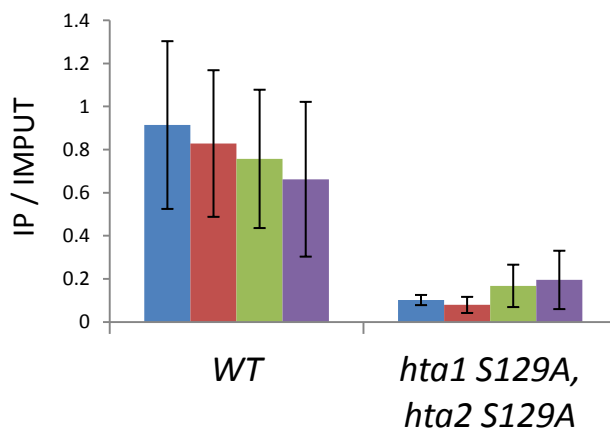


Figure 10. ChIP analysis for rDNA-NPC association in the histon H2A mutant

Figure 10. ChIP analysis for rDNA-NPC association in the histone H2A mutant

(a): Association of rDNA with the nuclear pore complex (NPC) analyzed by ChIP assays. NOY408-1b (WT, wild-type), the histone H2A mutant (*hta1 S129A*, *hta2 S129A*) were treated with formaldehyde and DNA associated with NPC was immunoprecipitated with an anti-NPC antibody. Four regions within rDNA (1 to 4 shown in Figure 4a) as well as control regions, one in telomere of Chr. XII and one in telomere of Chr. VI were analyzed by PCR. PCR products obtained for two sample concentrations (2-fold dilution) were separated on 1.8% agarose gels and stained with ethidium bromide. (b): PCR products shown in (Figure 4a) and other independent experiments were quantified. The values obtained for immunoprecipitated (IP) DNA were normalized to the values for corresponding input DNAs obtained without IP. Average values from three independent experiments are shown in arbitrary units. Error bars represent standard deviations (means \pm sd).

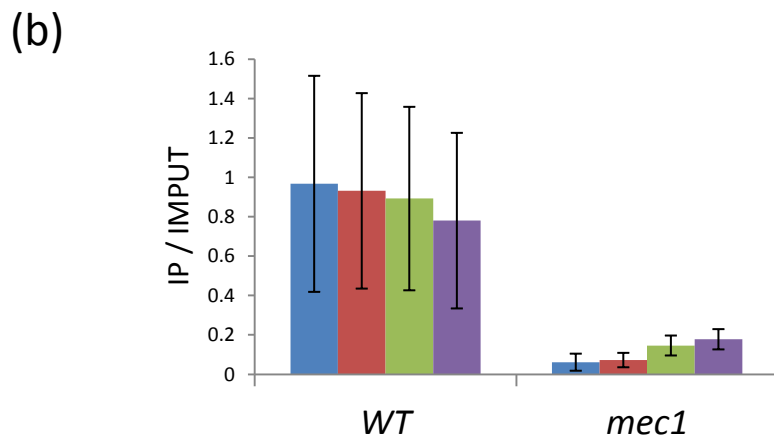
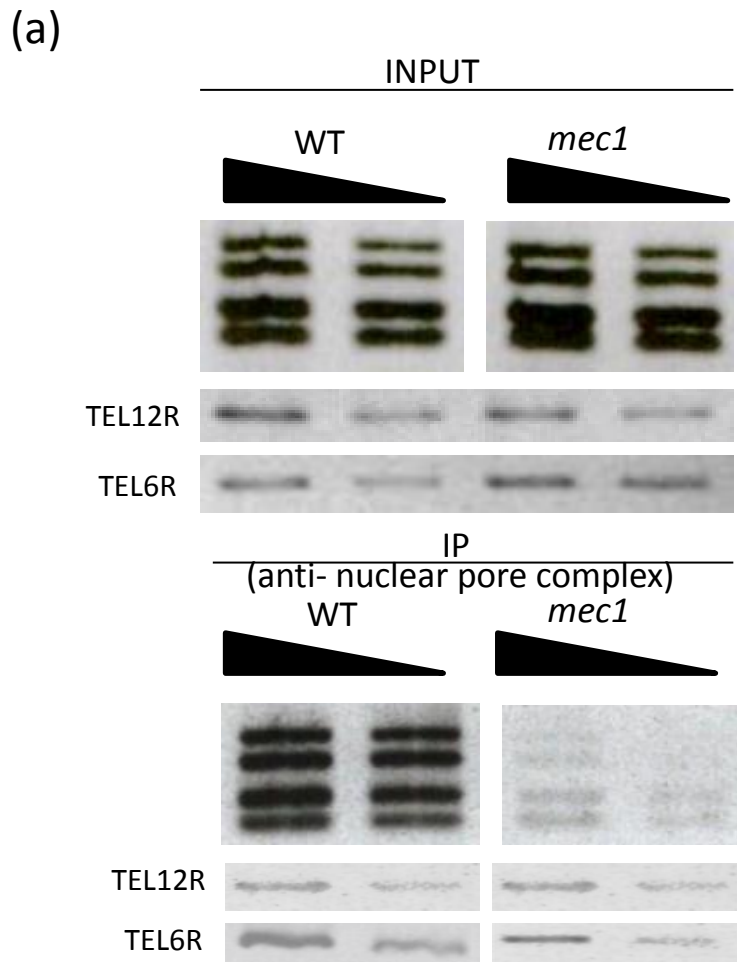


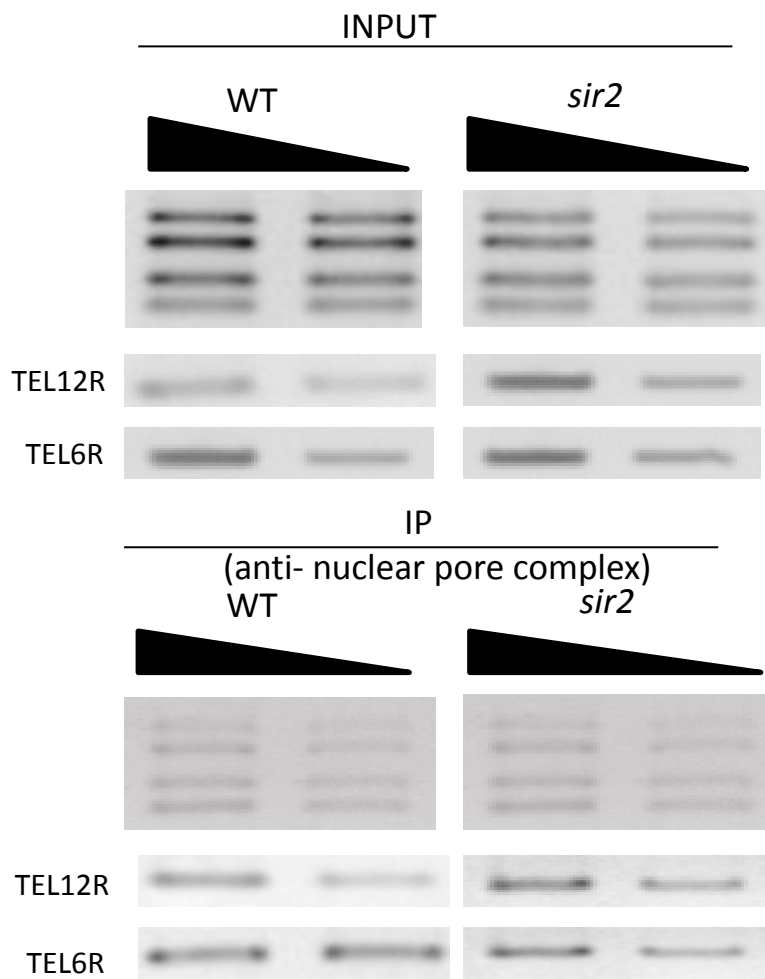
Figure 11. ChIP analysis for rDNA-NPC association in the *mec1* mutant

Figure 11. ChIP analysis for rDNA-NPC association in the *mec1* mutant

(a): Association of rDNA with the nuclear pore complex (NPC) analyzed by ChIP assays. NOY408-1b wild-type, the *mec1* mutant (*mec1*) were treated with formaldehyde and DNA associated with NPC was immunoprecipitated with an anti-NPC antibody. Four regions within rDNA (1 to 4 shown in Figure 4a) as well as control regions, one at telomere of Chr. XII and one at telomere of Chr. VI were analyzed by PCR. PCR products obtained for two sample concentrations (2-fold dilution) were separated on 1.8% agarose gels and stained with ethidium bromide.

(b): PCR products shown in (Figure 4a) and other independent experiments were quantified. The values obtained for immunoprecipitated (IP) DNA were normalized to the values for corresponding input DNAs obtained without IP. Average values from three independent experiments are shown in arbitrary units. Error bars represent standard deviations (means \pm sd).

(a)



(b)

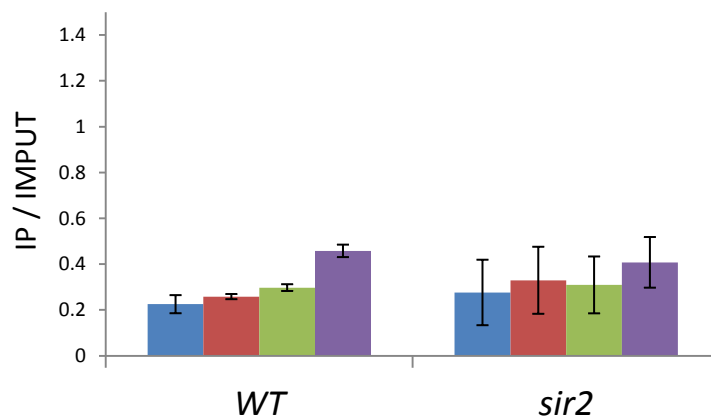


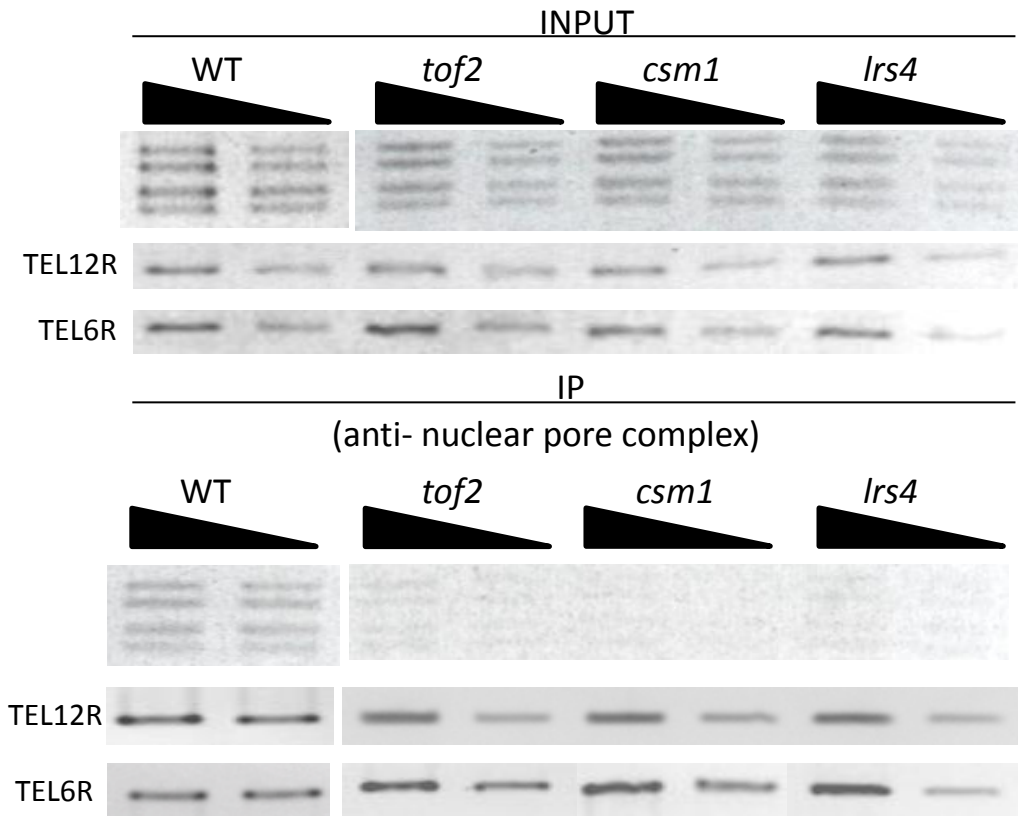
Figure 12. ChIP analysis for rDNA-NPC association in the *sir2* mutant

Figure 12. ChIP analysis for rDNA-NPC association in the *sir2* mutant

(a): Association of rDNA with the nuclear pore complex (NPC) analyzed by ChIP assays. NOY408-1b (WT, wild-type), the *sir2* mutant (*sir2*) were treated with formaldehyde and DNA associated with NPC was immunoprecipitated with an anti-NPC antibody. Four regions within rDNA (1 to 4 shown in Figure 4a) as well as control regions, one at telomere of Chr. XII and one at telomere of Chr. VI were analyzed by PCR. PCR products obtained for two sample concentrations (2-fold dilution) were separated on 1.8% agarose gels and stained with ethidium bromide.

(b): PCR products shown in (Figure 4a) and other independent experiments were quantified. The values obtained for immunoprecipitated (IP) DNA were normalized to the values for corresponding input DNAs obtained without IP. Average values from three independent experiments are shown in arbitrary units. Error bars represent standard deviations (means \pm sd).

(a)



(b)

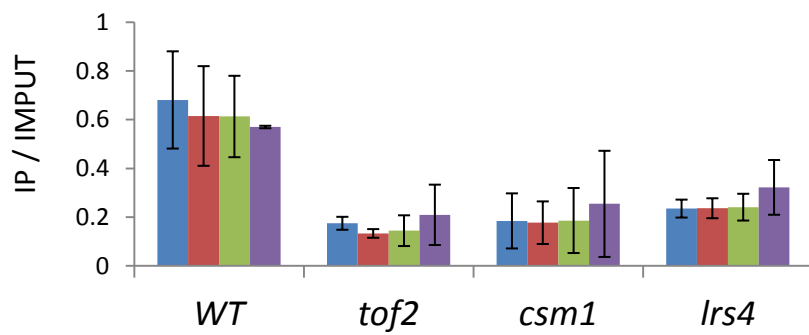


Figure 13. ChIP analysis for rDNA-NPC associations in condensin recruit factor mutants

Figure 13. ChIP analysis for rDNA-NPC associations in condensin recruit factor mutants

(a): Association of rDNA with the nuclear pore complex (NPC) analyzed by ChIP assays. NOY408-1b (WT, wild-type), the *tof2* mutant (*tof2*), the *csml* mutant (*csml*), the *lrs4* mutant (*lrs4*) were treated with formaldehyde and DNA associated with NPC was immunoprecipitated with an anti-NPC antibody. Four regions within rDNA (1 to 4 shown in Figure 4a) as well as control regions, one at telomere of Chr. XII and one at telomere of Chr. VI were analyzed by PCR. PCR products obtained for two sample concentrations (2-fold dilution) were separated on 1.8% agarose gels and stained with ethidium bromide. (b): PCR products shown in (Figure 4a) and other independent experiments were quantified. The values obtained for immunoprecipitated (IP) DNA were normalized to the values for corresponding input DNAs obtained without IP. Average values from three independent experiments are shown in arbitrary units. Error bars represent standard deviations (means \pm sd).

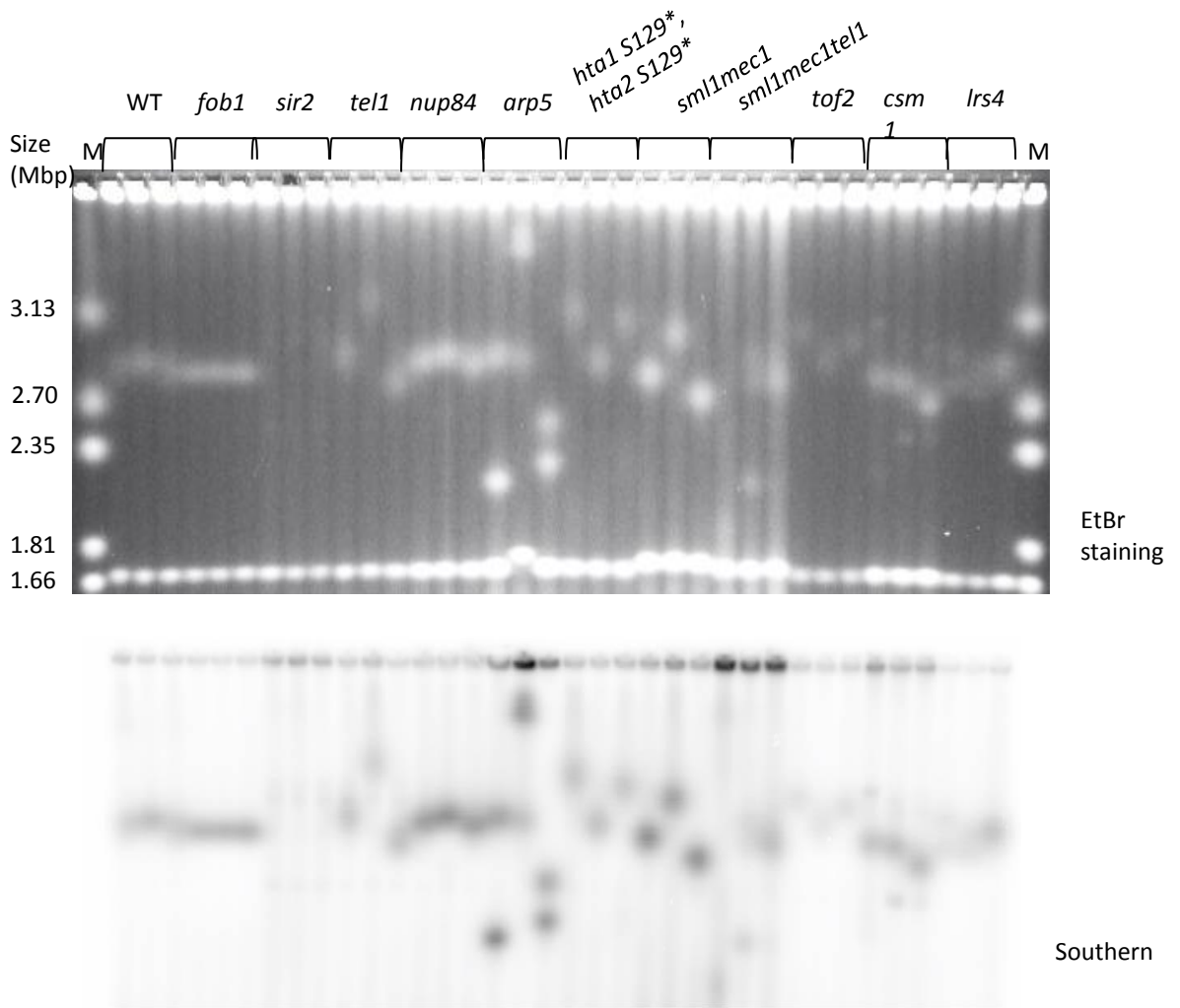
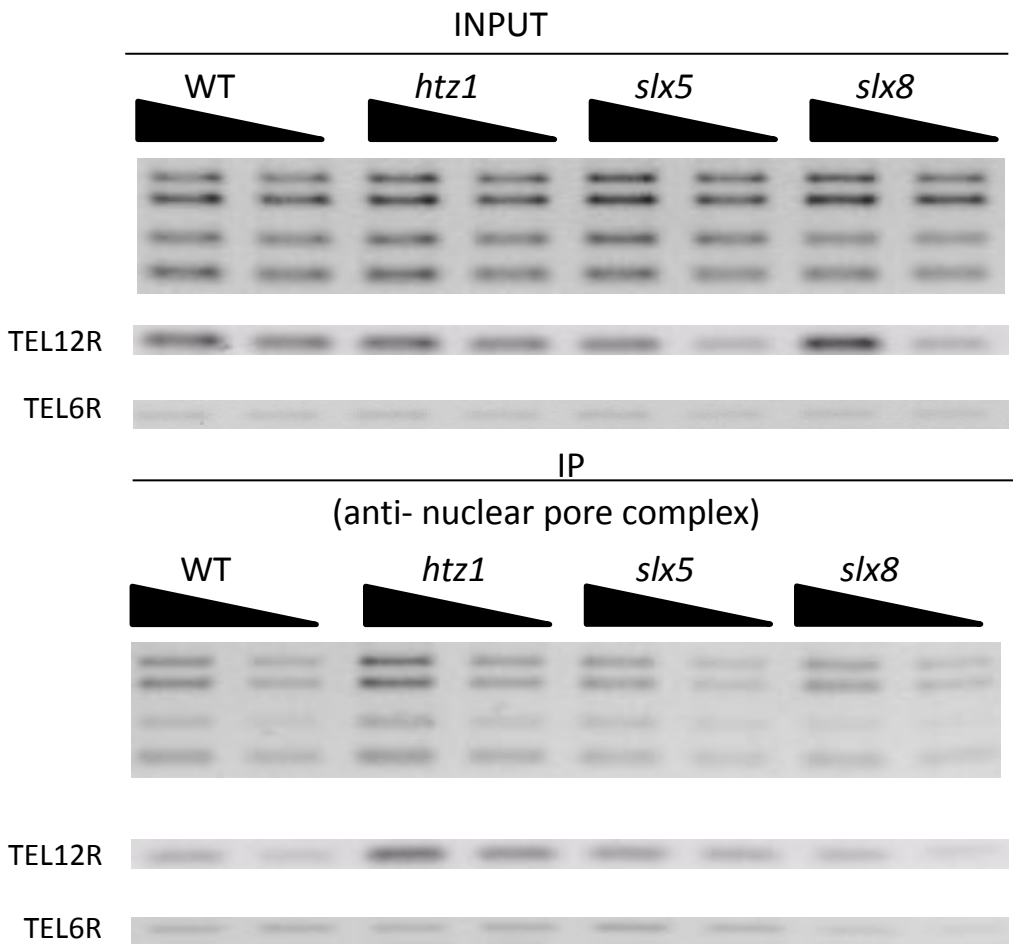


Figure 14. CHEF analysis of rDNA stability in mutants of genes involved in the transport of DSB in the rDNA to the nuclear pore

Figure 14. CHEF analysis of rDNA stability in mutants of genes involved in the transportation of DSB in the rDNA to the nuclear pore complex.

Top and bottom: ethidium bromide (EtBr) staining of Chr. XII and other chromosomes. Chromosomes from *S. cerevisiae* cells grown to saturation were resolved on a 1.0% CHEF gel for 68h and ethidium bromide stained. The yeast *Hansenula wingei* was served as size marker.

(a)



(b)

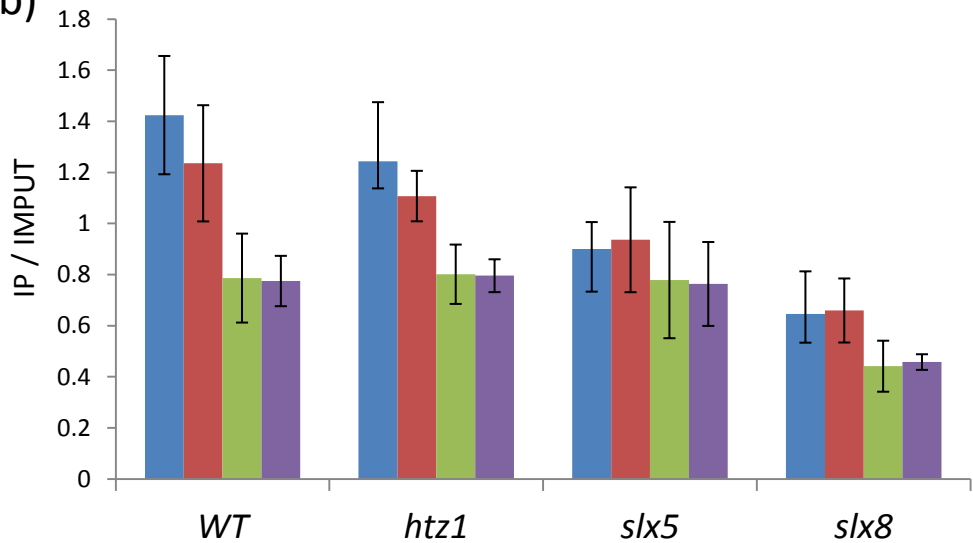


Figure 15. ChIP analysis for rDNA-NPC association in the *htz1* mutant, the *slx5* mutant and the *slx8* mutant.

Figure 15. ChIP analysis for rDNA-NPC association in the *htz1* mutant, the *slx5* mutant and the *slx8* mutant.

(a): Association of rDNA with the nuclear pore complex (NPC) analyzed by ChIP assays. NOY408-1b wild-type, the *htz1* mutant, the *slx5* mutant and the *slx8* mutant were treated with formaldehyde and DNA associated with NPC was immunoprecipitated with an anti-NPC antibody. Four regions within rDNA (1 to 4 shown in Figure 4a) as well as control regions, one at telomere of Chr. XII and one at telomere of Chr. VI were analyzed by PCR. PCR products obtained for two sample concentrations (2-fold dilution) were separated on 2.0% agarose gels and stained with ethidium bromide. (b): PCR products shown in (Figure 4a) and other independent experiments were quantified. The values obtained for immunoprecipitated (IP) DNA were normalized to the values for corresponding input DNAs obtained without IP. Average values from three independent experiments are shown in arbitrary units. Error bars represent standard deviations (means \pm sd).

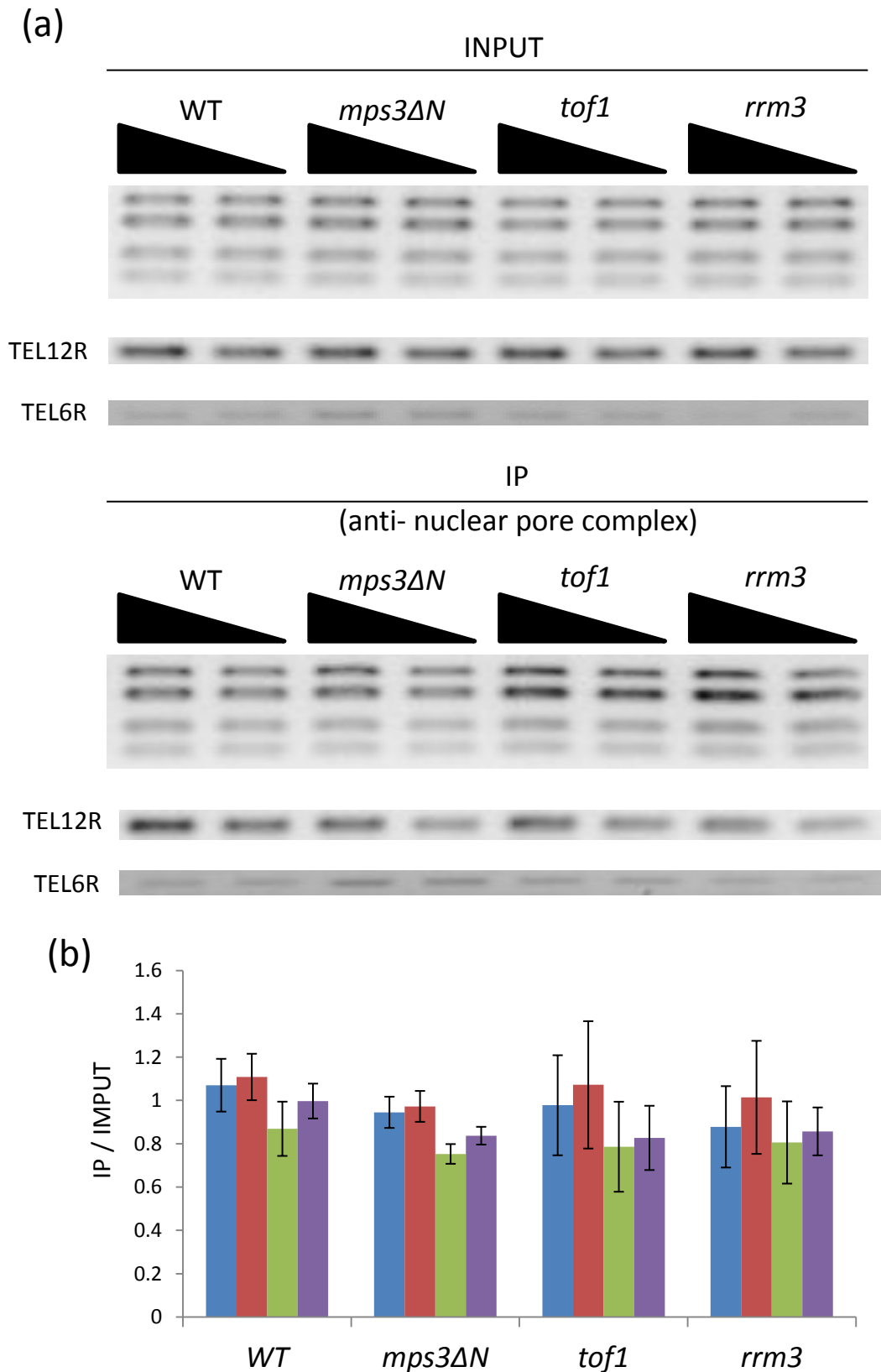


Figure 16. ChIP analysis for rDNA-NPC associations in the N-terminal Mps3 mutant, the *tof1* mutant and the *rrm3* mutant

Figure 16. ChIP analysis for rDNA-NPC associations in the N-terminal Mps3 mutant, the *tof1* mutant and the *rrm3* mutant

(a): Association of rDNA with the nuclear pore complex (NPC) analyzed by ChIP assays. NOY408-1b (WT, wild-type), the N-terminal Mps3 mutant (*mps3ΔN*), the *tof1* mutant and the *rrm3* mutant were treated with formaldehyde and DNA associated with NPC was immunoprecipitated with an anti-NPC antibody. Four regions within rDNA (1 to 4 shown in Figure 4a) as well as control regions, one at telomere of Chr. XII and one at telomere of Chr. VI were analyzed by PCR. PCR products obtained for two sample concentrations (2-fold dilution) were separated on 1.8% agarose gels and stained with ethidium bromide. (b): PCR products shown in (Figure 4a) and other independent experiments were quantified. The values obtained for immunoprecipitated (IP) DNA were normalized to the values for corresponding input DNAs obtained without IP. Average values from three independent experiments are shown in arbitrary units. Error bars represent standard deviations (means \pm sd).

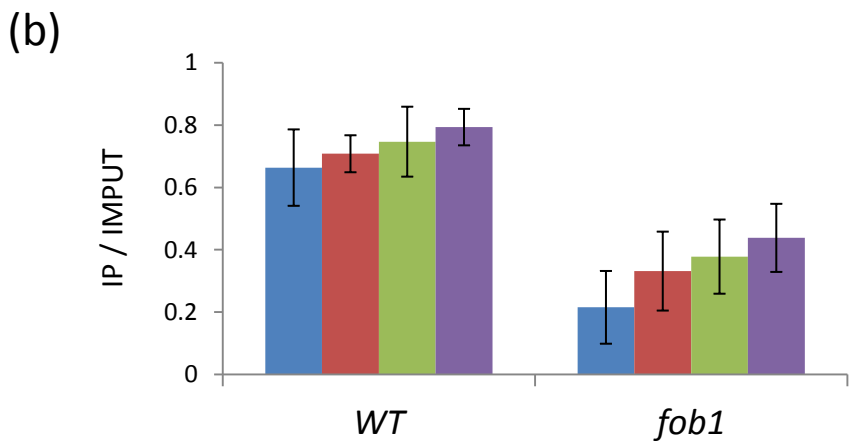


Figure 17. ChIP analysis for rDNA-Mps3 associations in strain with FLAG tag in the C-terminus of Mps3

Figure 17. ChIP analysis for rDNA-Mps3 associations in strains with FLAG tag in the C-terminus of Mps3

(a): Association of rDNA with Nup84, which is component of NPC, analyzed by ChIP assays. ChIPs were carried out in NOY408-1b (WT, wild type) and the *fob1* mutant (*fob1Δ*) added FLAG tag in the C-terminus of Mps3, respectively. *HIS3* gene was used as marker gene for transformation to add FLAG tag. These cells were treated with formaldehyde and DNA associated with Mps3 was immunoprecipitated with an anti-FLAG antibody. Four regions within rDNA (1 to 4 shown in Figure 4a) as well as control regions, one at telomere of Chr. XII and one at telomere of Chr. VI were analyzed by PCR. PCR products obtained for two sample concentrations (2-fold dilution) were separated on 1.8% agarose gels and stained with ethidium bromide. (b): PCR products shown in (Figure 4a) and other independent experiments were quantified. The values obtained for immunoprecipitated (IP) DNA were normalized to the values for corresponding input DNAs obtained without IP. Average values from three independent experiments are shown in arbitrary units. Error bars represent standard deviations (means \pm sd).

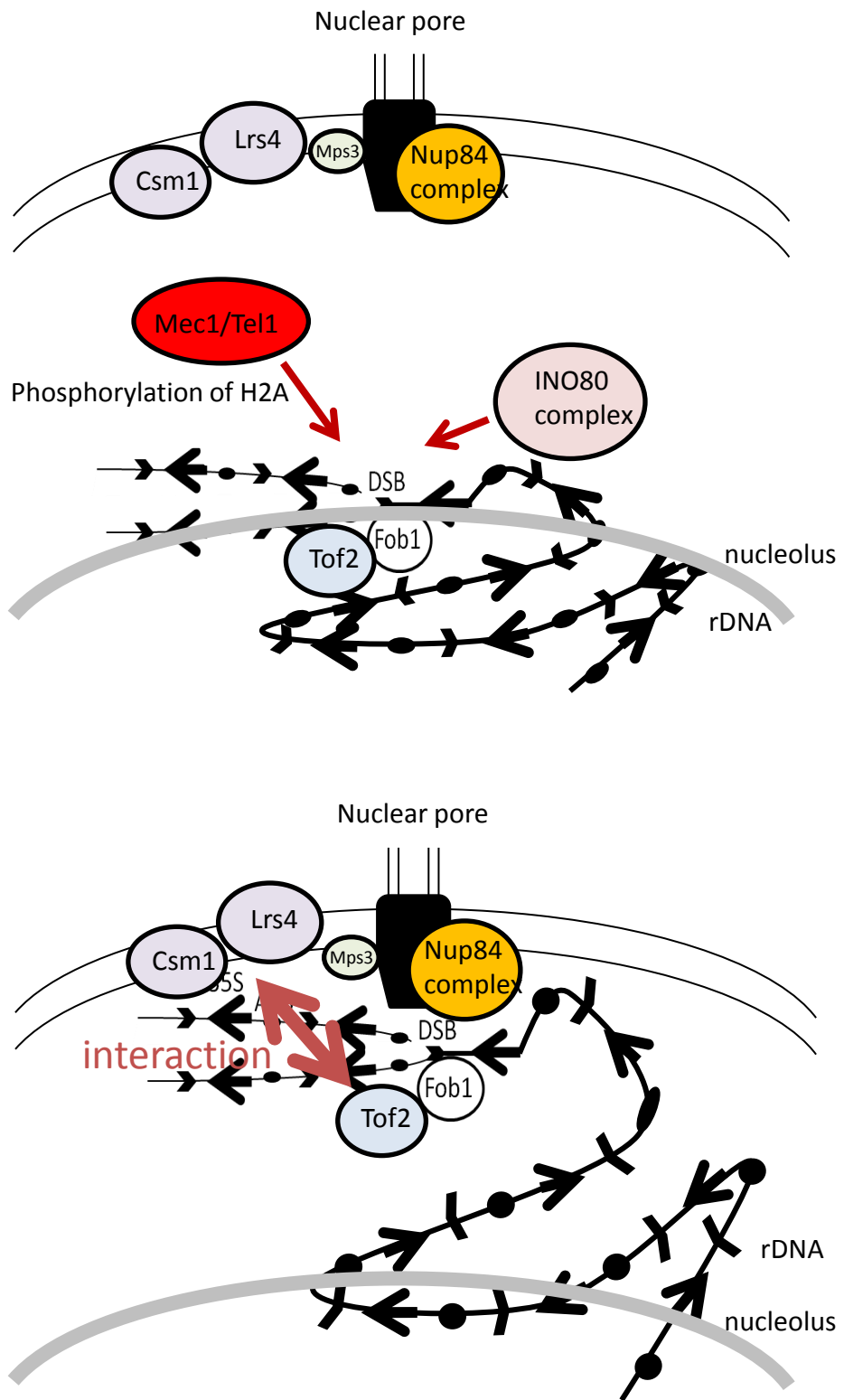


Figure 18. The model of the transportation of the rDNA to the NPC

Figure 18. The model of the transportation of the rDNA to the NPC.

DSB is induced at the RFB site in the rDNA, Mec1/Tel1 phosphorylates histone H2A, Ino80 complex is recruited to the phosphorylated histone H2A, and after that, DSB in the rDNA is recruited to the NPC. Condensin recruiters (Tof2, Csm1, Lrs4) to the RFB is required for the transportation of the rDNA to the NPC. The transportation has a role to avoid recombination with improper copies.